CHAPTER III

RESULTS

3.1 Procurement of the target sequence and designing the 2LTRZFP

To target the HIV-1 DNA sequence of 2-LTR-circle junctions, the DNA sequence covering the 2-LTR-circle junctions was submitted to the Zinc Finger Tools using "Search DNA Sequence for Contiguous Target Sites" mode. Eight candidate DNA sequences were obtained and the binding prediction scores of these sequences are detailed in **Table 3.1**. The sequence (5' CTAGCAGTACTGGATGGG 3') that had the highest score (60.65) with no potential target site overlap was selected for further designing the ZFP to obtain the most specific binding activity.

The design tool showed the amino acid sequence in α-helix of each finger predicted to bind to the triplet DNA target at 2-LTR-circle junctions **(Table 3.2)** and pop-up ELISA graphs for predicted binding activity in each finger to triplet DNA target were shown in **Figure 3.1**. The full-length amino acid sequence of designed ZFP was generated and designated namely 2LTRZFP. This protein was comprised of 176 amino acids for a six-zinc finger motif as shown in **Figure 3.2**. The amino acid sequence of 2LTRZFP was reverse-translated into a nucleotide sequence, and all codons in this sequence were optimized as demonstrated in **Figure 3.2**. The full-length optimized sequence was sent for full-gene synthesis by Blue Heron Biotechnology. Predicted properties of the resulting proteins were computed using ExPaSy proteomics tools. The resulting theoretical pI/Mw was 9.46 / 20.1 kDa

Prediction of the protein subcellular localization using the LOCtree program indicated that 2LTRZFP is a nuclear protein and is found in the nucleus.

Table 3.1 The results of searching for zinc finger target sites at HIV-1 DNA sequence of 2-LTR-circle junctions.

No.	Score	TSO	Target sequence (5' to 3')
1*	60.65	No	CTA GCA GTA CTG GAT GGG
2*	60.65	Yes	GCA GTA CTG GAT GGG CTA
3*	60.28	Yes	GTA CTG GAT GGG CTA ATT
4*	53.22	No	AGC AGTxACT GGA TGG GCT
5*	53.55	No	AGTxACT GGA TGG GCT AAT
6**	57.85	No	GCC CAT CCA GTA CTG CTA
7**	57.53	No	CAT CCA GTA CTG CTA GAG
8**	59.29	Yes	CCA GTA CTG CTA GAG ATT

*Searched from forward strand

** Searched from reverse strand

TSO; Target site overlap (colored in red)

Green highlight represent sequence of U5 of 3'LTR

Yellow highlight represent sequence of U3 of 5'LTR

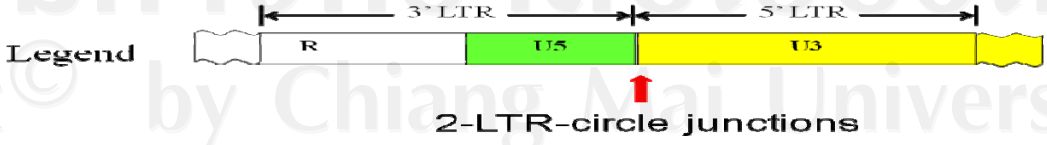

Table 3.2 The amino acid sequence in α-helix of each finger predicted to bind to the triplet DNA target at 2-LTR-circle junctions.

Finger	Triplet	α-Helix
1	**GGG**	**RSDKLVR**
2	**GAT**	**TSGNLVR**
3	**CTG**	**RNDALTE**
4	**GTA**	**QSSSLVR**
5	**GCA**	**QSGDLRR**
6	**CTA**	**QNSTLTE**

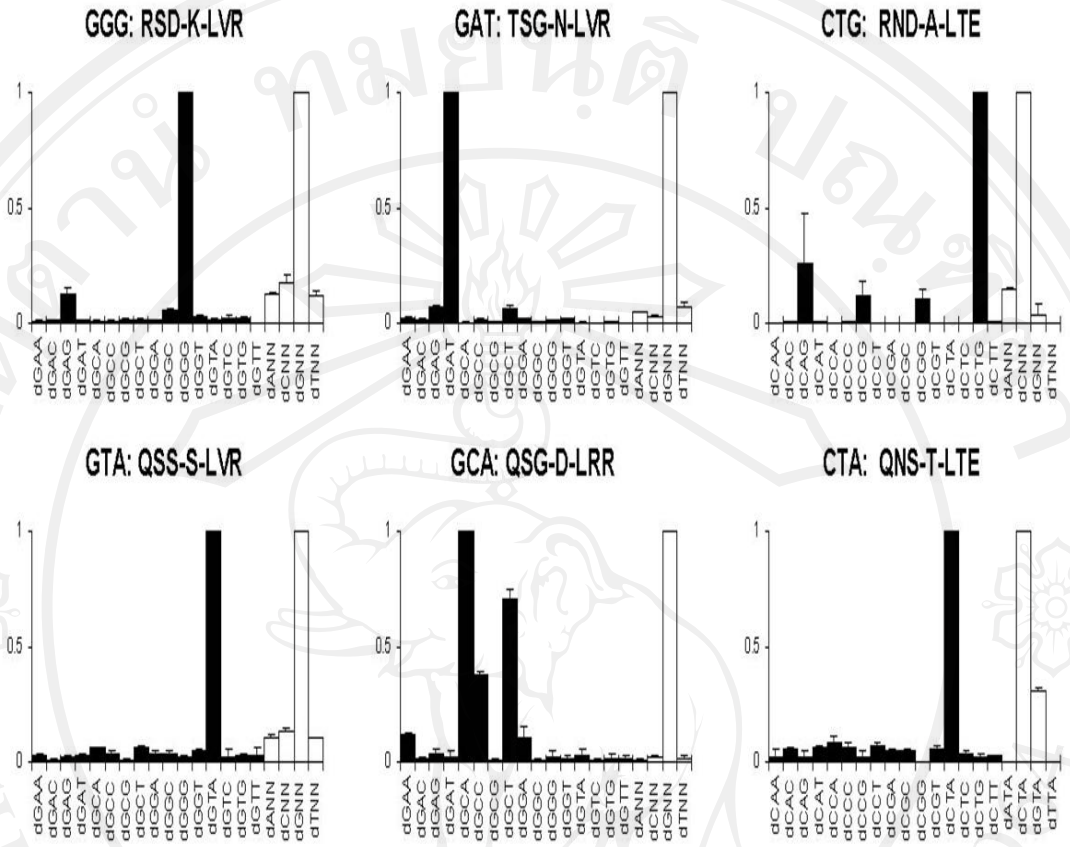

Figure 3.1 The pop-up ELISA graphs for predicted binding activity in each finger to triplet DNA target (Segal et al., 1999; Dreier et al., 2000; Mandell and Barbas, 2006). At the top of each graph is the recognition helix for each finger (positions -1 to 6). Position 3 is flanked by dash marks (-) for clarity. Black bars represent the binding activity of each finger with target oligonucleotides. White bars represent the binding activity of each finger with oligonucleotide pools with a particular 5' nucleotide subsite: GNN, ANN, TNN, and CNN. The height of each bar represents the relative specificity of the protein for each target, averaged over two independent experiments and normalized to the highest signal among the black or white bars. Error bars represent the deviation from the average.

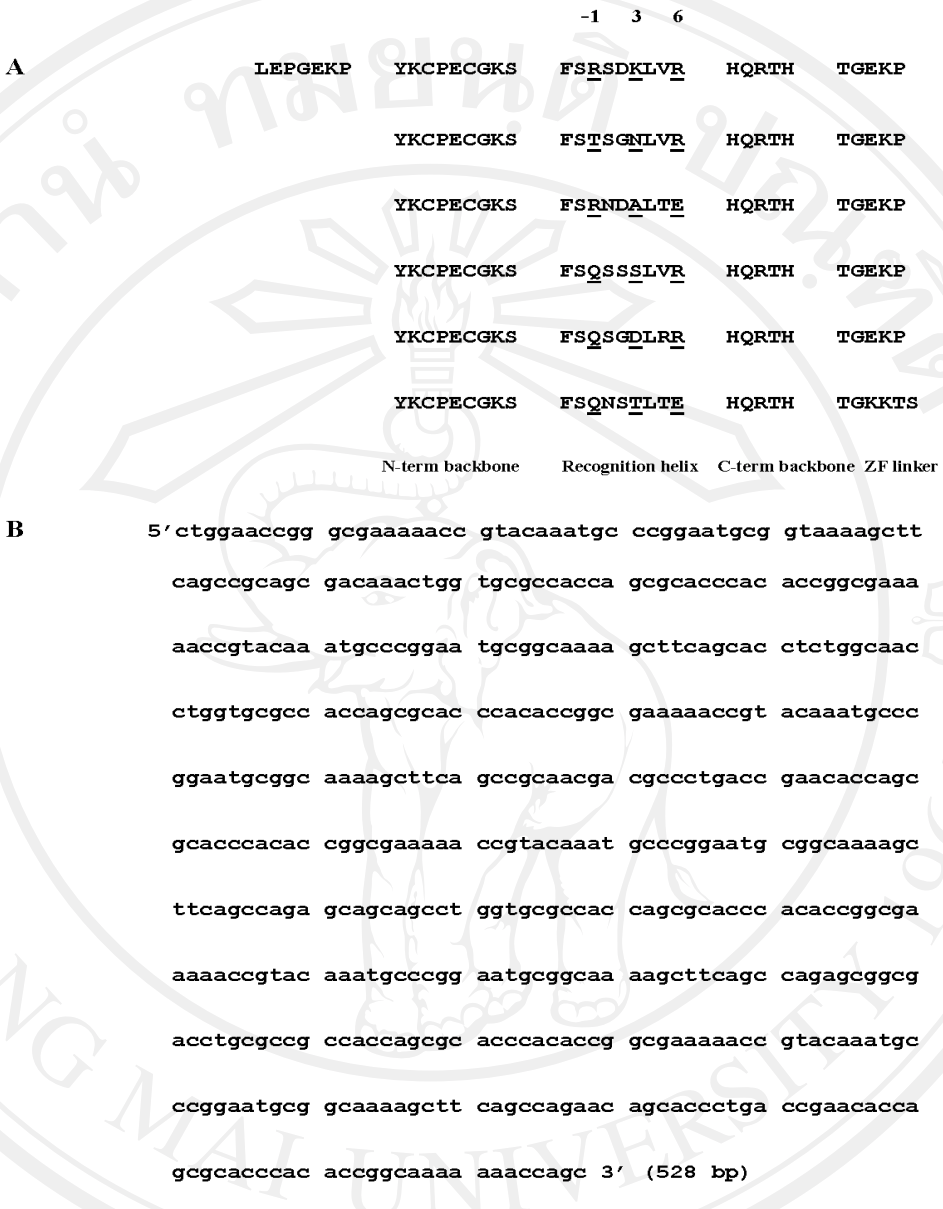

Figure 3.2 Full-length amino acid and optimized nucleotide sequence of 2LTRZFP. (A) Full-length amino acid sequence of 2LTRZFP. The amino acids shown by underline were located at the specific positions of -1, 3, and 6 from the N-terminal of the α-helix, respectively. N-terminal backbone: YKCPECGKSFS C-terminal backbone: HQRTH, ZF linker: TGEKP, N-terminal fixed: LEPGEKP, C-terminal fixed: TGKKTS **(B)** Full-length optimized nucleotide sequence of 2LTRZFP**.**

3.2 Construction of pTriEx-4- 2LTRZFP-GFP

The restriction endonucleases *Xcm*I and *Sma*I in the plasmid vector pTriEx-4-GFP was used as a cloning sites for the 2LTRZFP gene fragment to construct the pTriEx-4-2LTRZFP-GFP containing His6 at N-terminal and fused-GFP at C-terminal under the control of the CMV, T7, or p10 promoters as shown in **Figure 3.3**. The plasmid vector pTriEx-4-2LTRZFP-GFP was digested by the restriction endonucleases *Xcm*I and *Sma*I and the product was subjected to 1 % agarose gel electrophoresis and visualized by ethidium bromide staining. Restriction digest analysis showed that the pTriEx-4-2LTRZFP-GFP was constructed successfully at a 547 bp band as seen in **Figure 3.4**.

3.3 Protein expression and purification

Protein construction of 2LTRZFP-GFP containing His6 at N-terminal and fused-GFP at C-terminal including thrombin cleavage site between 2LTRZFP and GFP was shown in **Figure 3.5 A**. It was expressed in its recombinant forms in *E. coli* Origami B (DE3) Novagen (Madison, WI). GFP can be observed under fluorescent microscope **(Figure 3.5 B)**. Protein purification was performed by using His-Bind column chromatography **(Figure 3.5 C)**. The entire expression and purification processes were monitored by SDS-PAGE as demonstated in **Figure 3.6 A**. Comparison between lane 2 [total lysate of *E. coli* Origami B (DE3)] and lane 3 [Total lysate of *E. coli* Origami B (DE3) with pTriEx-4-2LTRZFP-GFP was induced by IPTG after O.D. $_{600}$ reach 1.0 at 30 °C for overnight] indicates that the expression of fusion protein His6-2LTRZFP-GFP (approximately 50 kDa) was successful. In lane 6 show that this fusion protein bound to the His-Bind column chromatography

and it can be eluted by elution buffer containing 1 M imidazole, 0.5 M NaCl, 20 mM Tris-HCl, pH 7.9 (lane 7). Western blotting was performed by using anti-His mAb as primary antibody and the analysis demonstrated that His6-2LTRZFP-GFP (approximately 50 KDa) was successfully expressed as shown in **Figure 3.6 B**.

3.4 Expression of 2LTRZFP-GFP in HeLa cells

To test the expression of the 2LTRZFP-GFP recombinant protein in a mammalian system, pTriEx-4-2LTRZFP-GFP was transfected into a HeLa cell line. The emitted green fluorescence was observed under the microscope 24 and 48 h after transfection. The green fluorescence was observed in the nucleus in the pTriEx-4-2LTRZFP-GFP transfection group, and in the cytoplasm for pTriEx-4-GFP control group **(Figure 3.7)**. This result indicated that 2LTRZFP-GFP recombinant protein is a nuclear protein and confirmed the successful folding of the protein.

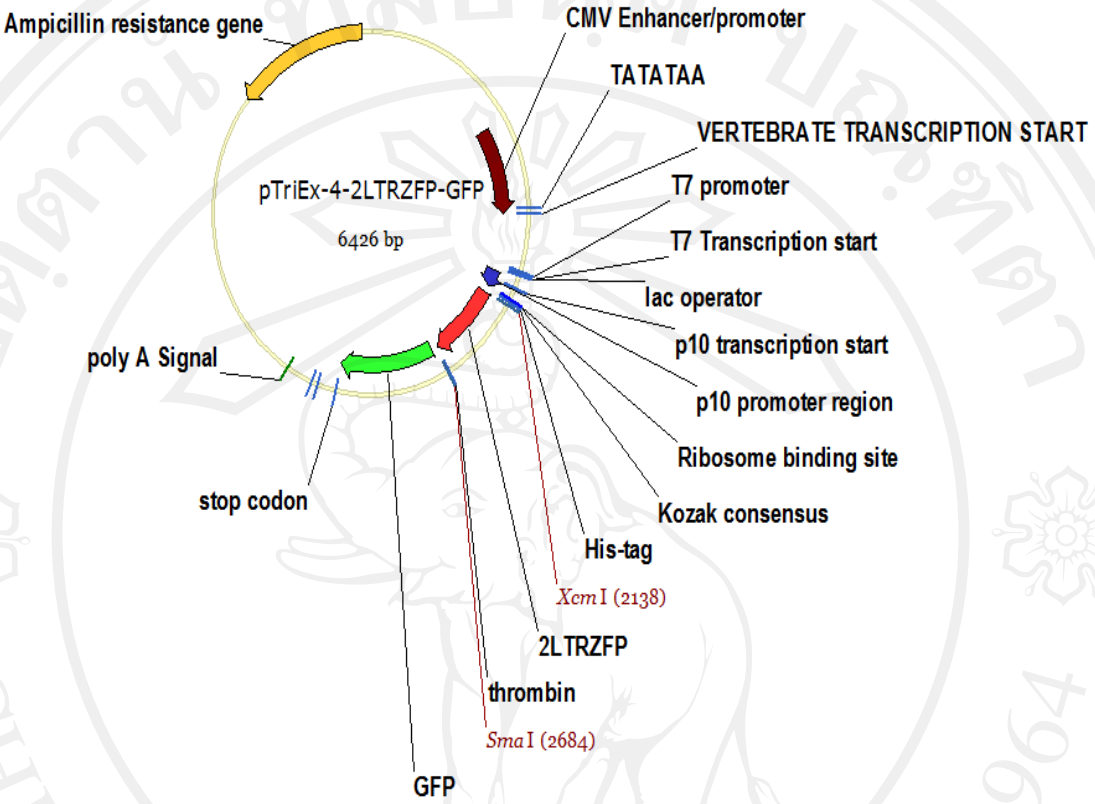

Figure 3.3 Construction of pTriEx-4- 2LTRZFP-GFP. The restriction endonucleases *Xcm*I and *Sma*I in the plasmid vector pTriEx-4-GFP was used as a cloning sites for the 2LTRZFP gene fragment to construct the pTriEx-4-2LTRZFP-GFP containing His6 at N-terminal and fused-GFP at C-terminal under the control of the CMV, T7, or p10 promoters.

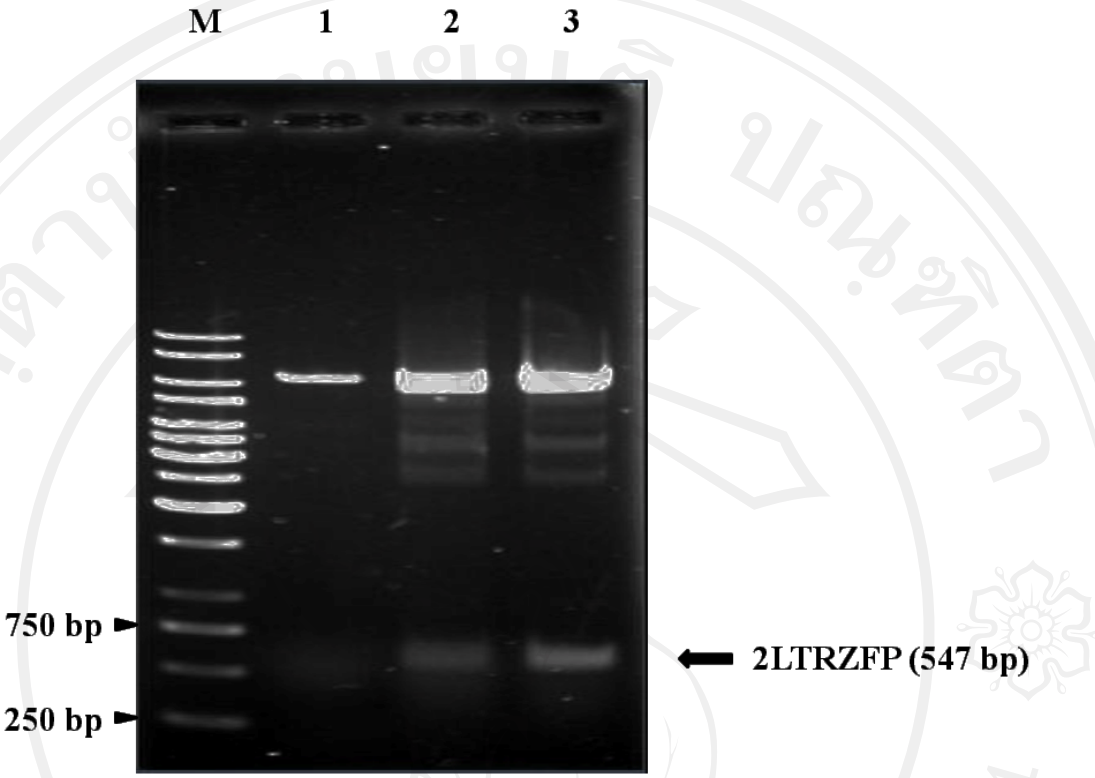

Figure 3.4 Restriction digest analysis of the pTriEx-4-2LTRZFP-GFP.

Lane M: 1 kb DNA ladder

Lane 1: pTriEx-4-2LTRZFP-GFP cut with *Xcm*I

Lane 2: pTriEx-4-2LTRZFP-GFP clone 1 cut with *Xcm*I and *Sma*I

Lane 3: pTriEx-4-2LTRZFP-GFP clone 2 cut with *Xcm*I and *Sma*I

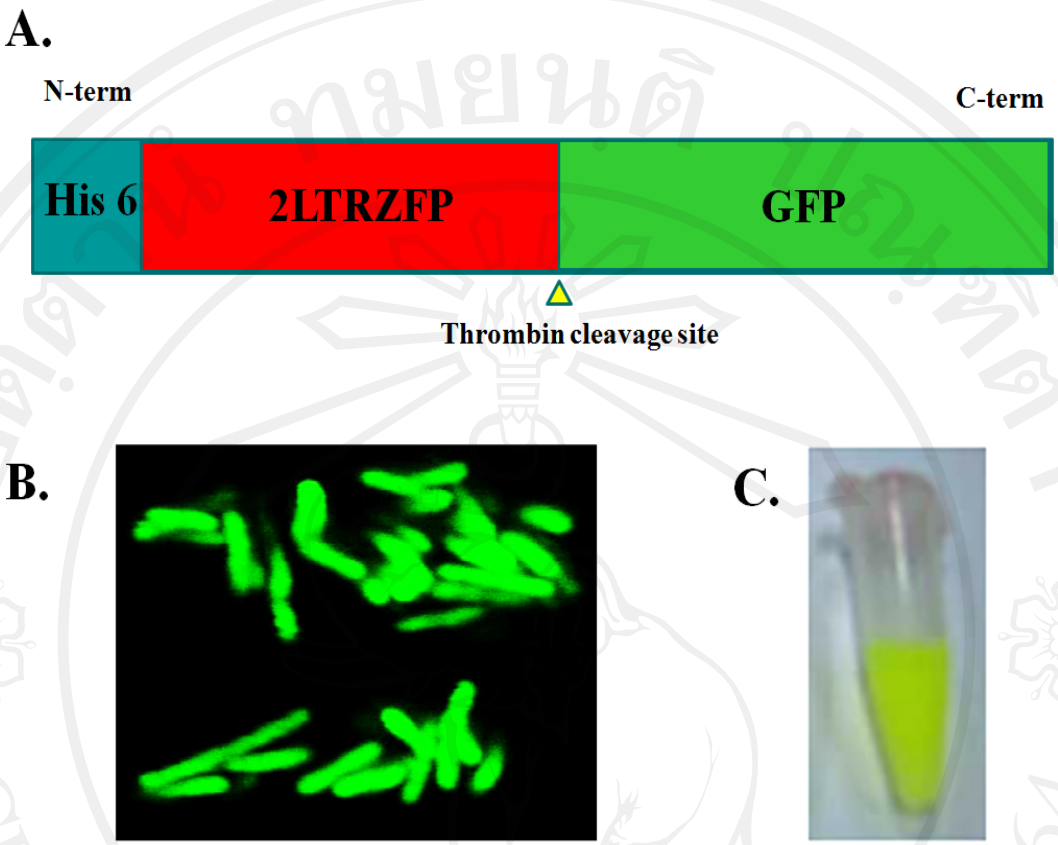

Figure 3.5 Protein construction and expression of 2LTRZFP-GFP. (A) Protein construction of 2LTRZFP-GFP. **(B)** Protein expression of 2LTRZFP-GFP in *E. coli* Origami B (DE3) and GFP was observed under fluorescent microscope. **(C)** The purified 2LTRZFP-GFP was prepared by using His-Bind column chromatography.

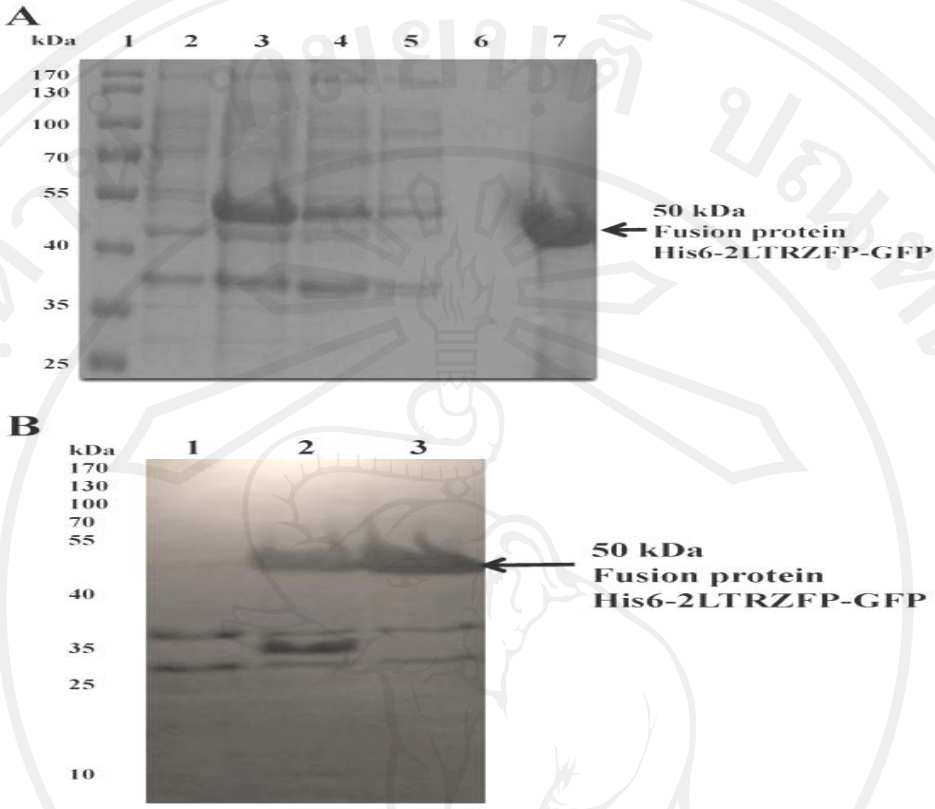

Figure 3.6 SDS-PAGE and Western blot analysis of His6-2LTRZFP-GFP.

(A) SDS-PAGE analysis of His6-2LTRZFP-GFP at different and purification steps. Lane 1. Protein marker, lane 2. Total bacterial lysate, lane 3. Total bacterial lysate with pTriEx-4-2LTRZFP-GFP after IPTG induction for overnight. lane 4. Pass-through lysate, lane 5 and 6. Solution after washing the column with binding buffer and washing buffer, respectively, lane 7. Elution of purified His6-2LTRZFP-GFP. The arrow indicates the size of 50 kDa of His6-2LTRZFP-GFP. Number on left show size in kilo Dalton of protein ladder. **(B)** Western blot analysis of His6-2LTRZFP-GFP at different condition of protein expression. Lane 1. Total bacterial lysate, lane 2 and 3. Total bacterial lysate with pTriEx-4-2LTRZFP-GFP after IPTG induction for 4 hr, and overnight, respectively. The arrow indicates the size of 50 kDa of His6-2LTRZFP-GFP. Number on left show size in kilo Dalton of protein ladder.

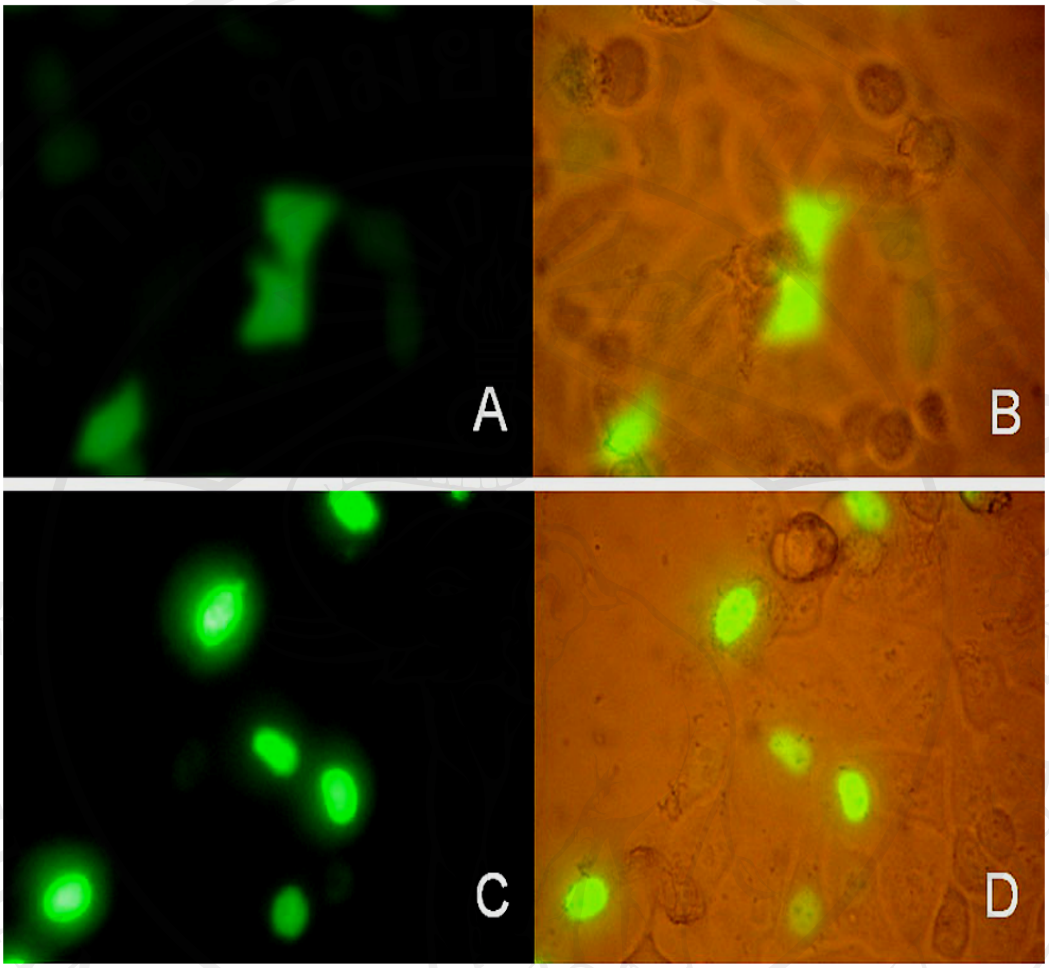

Figure 3.7 Expression of green fluorescent protein in HeLa cells 24 h after transfection. **(A and B)** Transfected with recombinant plasmid pTriEx-4-GFP. **(C and D)** Transfected with recombinant plasmid pTriEx-4-2LTRZFP-GFP. Each group was imaged at 400× magnification in the same field by inverted fluorescent microscope.

3.5 Evaluating of dissociation constants and competitive DNA binding activity by SPR

To determine real-time binding kinetics between 2LTRZFP-GFP and its target DNA sequence, SPR was used as a tool for affinity analysis. Different concentrations of 2LTRZFP-GFP were injected into the immobilized chip with specific ds-DNA. The 2LTRZFP-GFP could bind to its target ds-DNA on a nanomolar scale, with K_D = 12.0 nM as shown in **Figure 3.8**. A competitive SPR was also performed to determine the specificity of binding between 2LTRZFP-GFP and its target DNA. The concentration of 2LTRZFP-GFP (1.2 μM) was used to compete with 26.5 μM of non-biotinylated target ds-DNA and non-specific ds-DNA before injection onto the immobilized chip with specific ds-DNA. The 2LTRZFP-GFP could bind to its target DNA sequence (result compared with non-specific ds-DNA, as demonstrated in **Figure 3.9**. In addition, the specificity of binding activity was also assayed by injection of GFP and bovine serum albumin (BSA) as controls. These results demonstrated that the binding activity was involved with ZFP only **(Figure 3.8)**. To obtain the binding properties, the binding activity of 2LTRZFP-GFP and its target DNA sequence was also tested in zinc buffer containing of 1 μM, 1 mM, and 10 mM of EDTA. The binding activity was decreased when the concentration of EDTA was high. These findings supported the conclusion that the binding between 2LTRZFP-GFP and its target DNA sequence depended on zinc ions, and that this metal ion is important for stabilizing ZFP **(Figure 3.10)**.

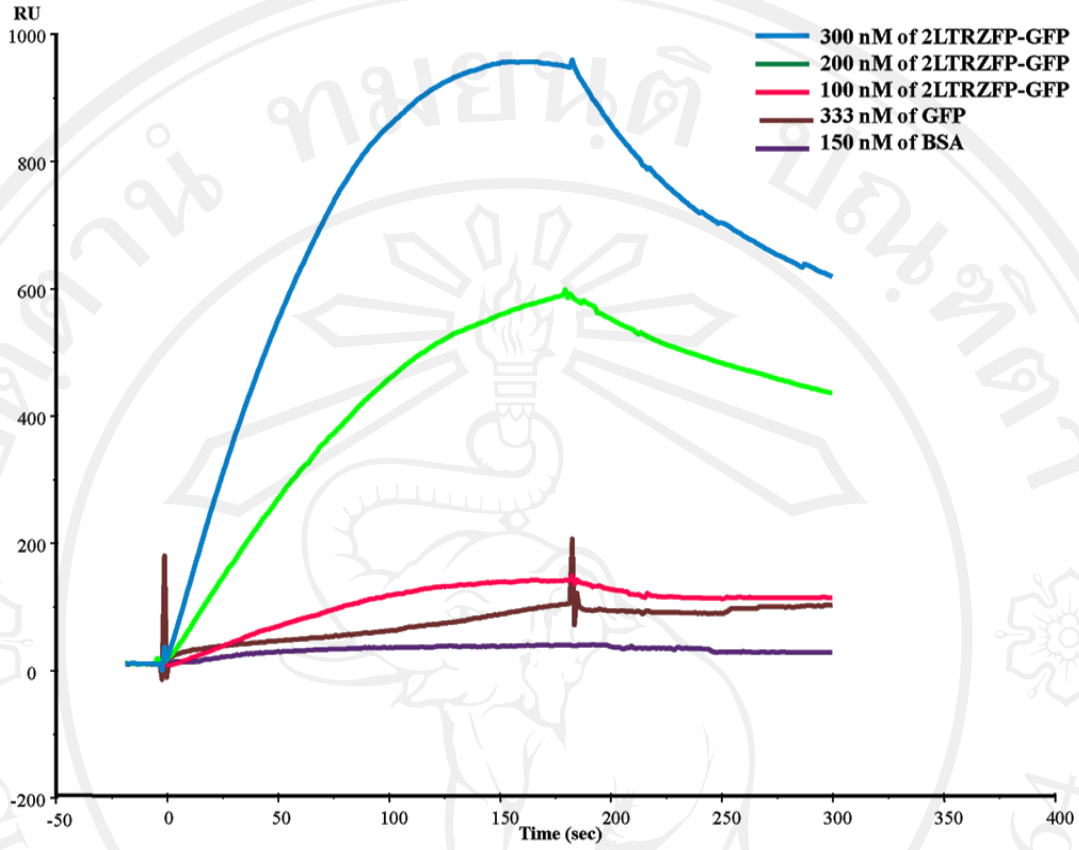

Figure 3.8 Kinetic binding analysis between 2LTRZFP-GFP and its target DNA sequence. 2LTRZFP-GFP (300, 200, and 100 nM), 333 nM of GFP and 150 nM of BSA was diluted in zinc buffer in a final volume 60 ul were injected to the immobilized chip with specific ds-DNA at a flow rate 20 ul/min, and followed by a dissociation phase of 180 s.

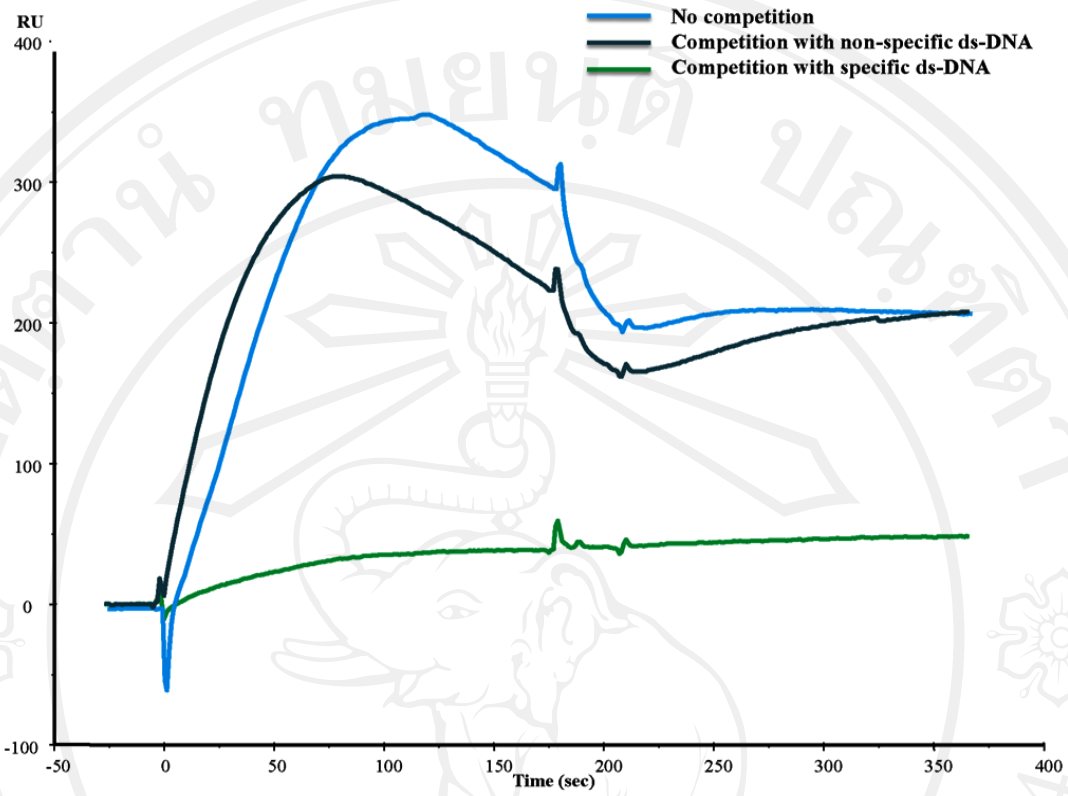

Figure 3.9 Kinetic binding analysis in the competitive SPR. 2LTRZFP-GFP was incubated with non-biotinylated ds-DNA of its target ds-DNA, and non-specific ds-DNA in zinc buffer for 15 min before injection.

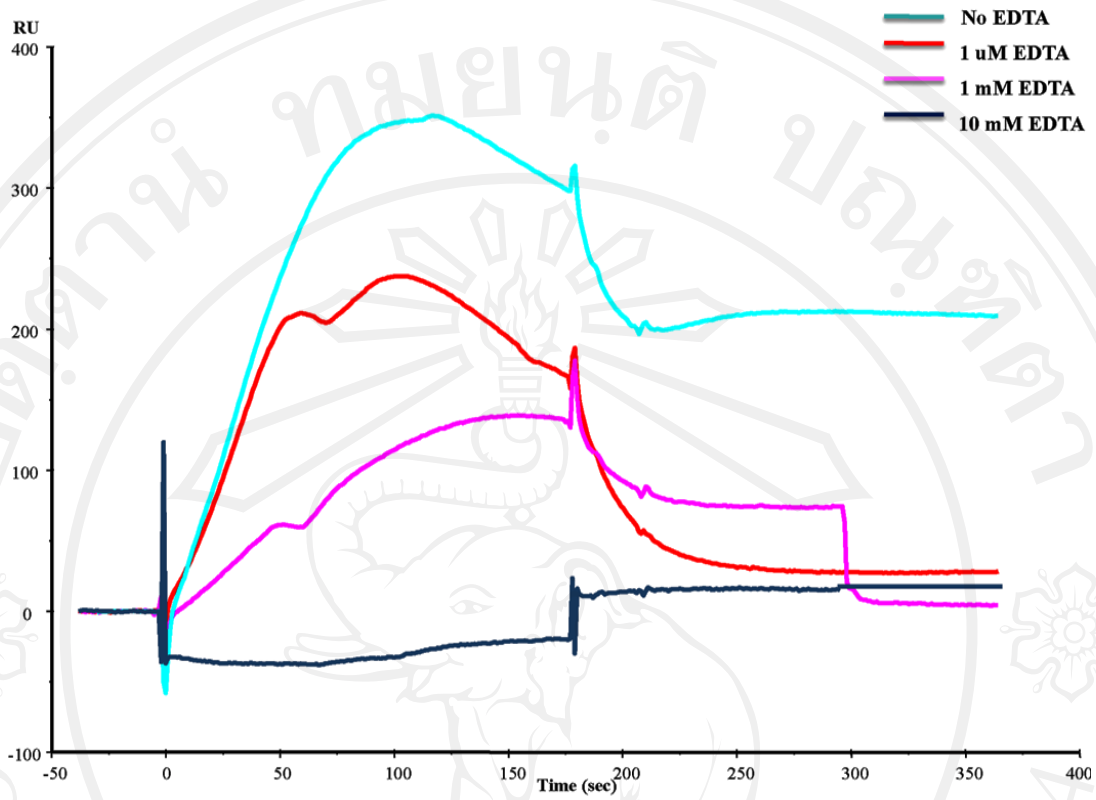

Figure 3.10 Kinetic binding of 2LTRZFP-GFP to its target DNA sequence depend on zinc ion. 2LTRZFP-GFP was injected to determine the binding activity with its target DNA sequence in zinc buffer containing of 1 µM, 1 mM, and 10 mM of EDTA.

3.6 DNA binding activity by EMSA

In order to confirm the binding activity, EMSA was performed using an EMSA kit as described in the materials and methods. A complete binding complex of 1 μM of 2LTRZFP-GFP and 250 nM of its specific DNA duplex could be observed (see **Figure 3.11A**, lane 8) until no band of free DNA duplex was seen. At the same time, a faint band of binding complex was observed in the reaction of 2LTRZFP-GFP and non-specific DNA duplex (**Figure 3.11A**, lane 9), whereas the intensity of free DNA duplex was not changed (**Figure 3.11A**, lanes 3 and 6). This experiment also demonstrated that GFP in 2LTRZFP-GFP recombinant protein was not involved in the binding (lanes 4, 5 and 6 of **Figure 3.11A**). The dilution effect of DNA binding complex can be observed in **Figure 3.11B and 3.11C**.

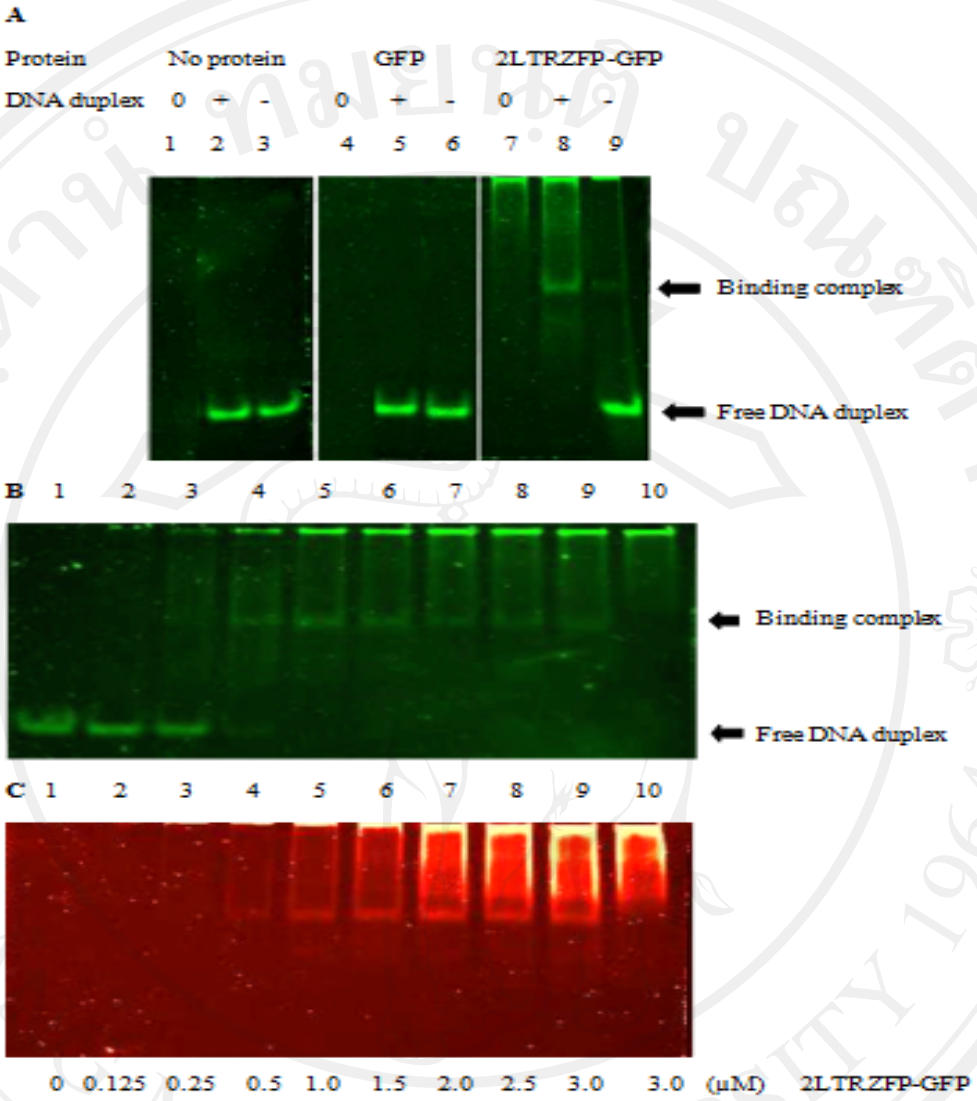

Figure 3.11 Electrophoretic mobility shift assay (EMSA). (A) The protein used for each reaction is 1 μM whereas [0], no DNA duplex; [+], specific DNA duplex; [-], non-specific DNA duplex. The gel was stained with SYBR® Green EMSA stain **(B)** or with SYPRO® Ruby EMSA stain **(C)**. In panel B and C: Lane 1 to 9, the specific DNA duplex used for each reaction was 250 nM, whereas 2LTRZFP-GFP was varied the concentration from 0, 0.125, 0.25, 0.5, 1.0, 1.5, 2.0, 2.5, 3.0 μM, respectively. Lane 10, 2LTRZFP-GFP was used 3.0 μM, but no DNA duplex.

3.7 Cloning of lentiviral-based vectors and non-viral vectors for stable line production

The *Xba*I and *Sal*I sites in the pRRLSIN.cPPT.mPGK-GFP.WPRE vector were used as cloning sites for 2LTRZFP-GFP, Aart-GFP, and RFP to construct pRRLSIN.cPPT.mPGK.2LTRZFP-GFP.WPRE, pRRLSIN.cPPT.mPGK.Aart-GFP.WPRE, and pRRLSIN.cPPT.mPGK-RFP.WPRE, respectively. Expression from these transgenes was controlled by the mPGK promoter (**Figure 3.12A**). The packaging vectors are schematically shown in (**Figure 3.12B**). The 2LTRZFP-GFP and Aart-GFP gene fragments were also cloned into the pCEP4 vector, and the flanking *Nhe*I and *Not*I sites were used to construct pCEP4-2LTRZFP-GFP and pCEP4-Aart-GFP to create N-terminal His6 and a C-terminal GFP fusions. The expression of genes in these plasmids was driven by the cytomegalovirus (CMV) immediate-early enhancer/promoter (**Figure 3.12C**). Restriction digest analysis showed that all constructions of lentiviral-based vectors **(Figure 3.13A and B),** and pCEP4-based vectors were cloned successfully as seen in **Figure 3.14**. All plasmids were confirmed by DNA sequencing.

3.8 Production and expression of VSV-G pseudotyped lentiviruses containing 2LTRZFP-GFP Aart-GFP, and RFP

VSV-G pseudotyped lentiviral particles carrying the 2LTRZFP-GFP, Aart-GFP, and RFP genes were produced by cotransfection in human embryonic kidney 293T cells using a four-component transient packaging vector system. This system was composed of the following components: 1) pMDLgag/polRRE in which the CMV immediate-early promoter drives the production of the gag/pol transcript

containing the Rev-responsive element (RRE); 2) pRSV-Rev, which encodes HIV-1 Rev; 3) pMD.G, which encodes the envelope G-protein of VSV; and 4) pRRLSIN.cPPT.mPGK-GFP.WPRE in which an expression cassette for the transgene is flanked by the *cis*-acting sequences necessary for packaging, reverse transcription, and integration, including the 5'- and 3'-LTRs (**Figure 3.12A**). High-titre virus stocks were harvested followed by the measurement of p24 Ag and the viral load. The results indicated the successful production of VSV-G pseudotyped lentiviruses containing 2LTRZFP-GFP Aart-GFP, and RFP (**Table 3.3**).

293T cells were transduced with VSV-G pseudotyped lentivirus containing 2LTRZFP-GFP, Aart-GFP, or RFP. Both 2LTRZFP-GFP and Aart-GFP were predominantly observed in the nucleus when the cells were observed by fluorescence microscopy, but RFP was homogeneously distributed throughout the cytoplasm and nucleus **(Figure 3.15**). To determine the effects of the long-term expression of 2LTRZFP-GFP and Aart-GFP in 293T cells, stably transfected cells grown for 90 days were analysed for GFP by flow cytometry. The percentages of cells containing 2LTRZFP-GFP and Aart-GFP in the stable 293T lines were 91 and 73 %, respectively as seen in **Figure 3.16**.

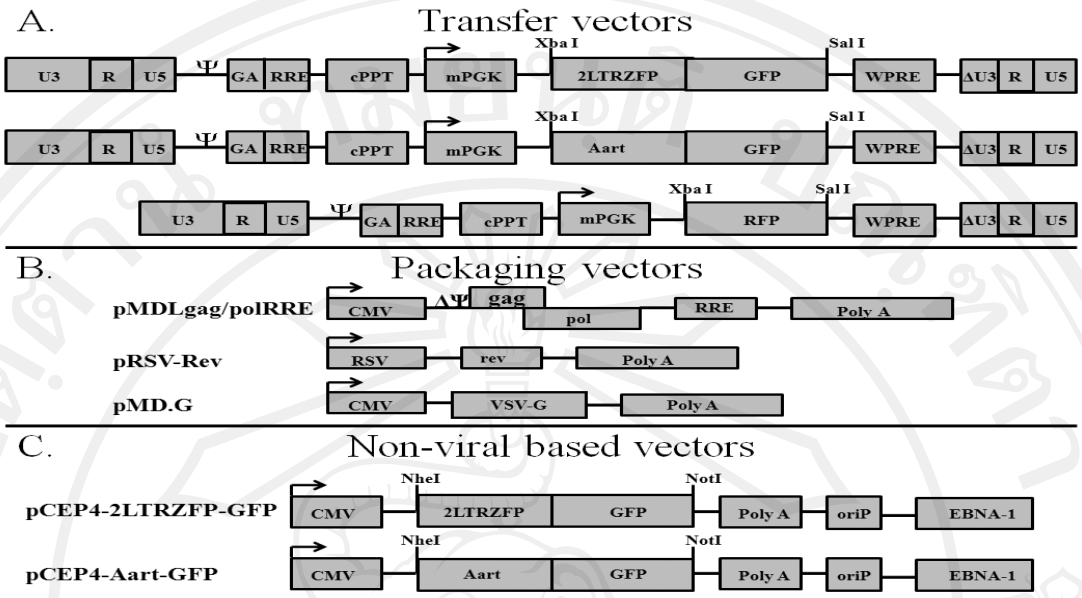

Figure 3.12 Schematic drawing of the expression vectors for 2LTRZFP-GFP, Aart-GFP, and RFP. (A) The transfer vectors used in this study were derived from the third-generation, self-inactivating vector pRRLSIN.cPPT.mPGK-GFP.WPRE. The *Xba*I and *Sal*I sites were used as the cloning sites for all transgenes. The following abbreviations are used: cPPT, central polypurine tract; GA, fragment of the HIV-1 *gag* gene; RRE, Rev responsive element; and WPRE, woodchuck hepatitis virus post-transcriptional regulatory element. **(B)** The packaging vector, pMDLgag/polRRE, expresses the *gag* and *pol* transcript, intervening sequences and polyadenylation site, and it is driven by the CMV promoter. pRSV-Rev expresses *rev* cDNA. pMD.G encodes a heterologous envelope to pseudotype the virus coding for VSV-G. **(C)** The non-viral based vector, pCEP4, was used to construct pCEP4-2LTRZFP-GFP and pCEP4-Aart-GFP for stable cell line production. *Nhe*I and *Not*I were used as cloning sites for both transgenes. The EBV origin of replication (oriP) and nuclear antigen (EBNA-1) signal result in high-copy episomal replication in primate and canine cell lines (Yates et al., 1985; Reisman and Sugden, 1986).

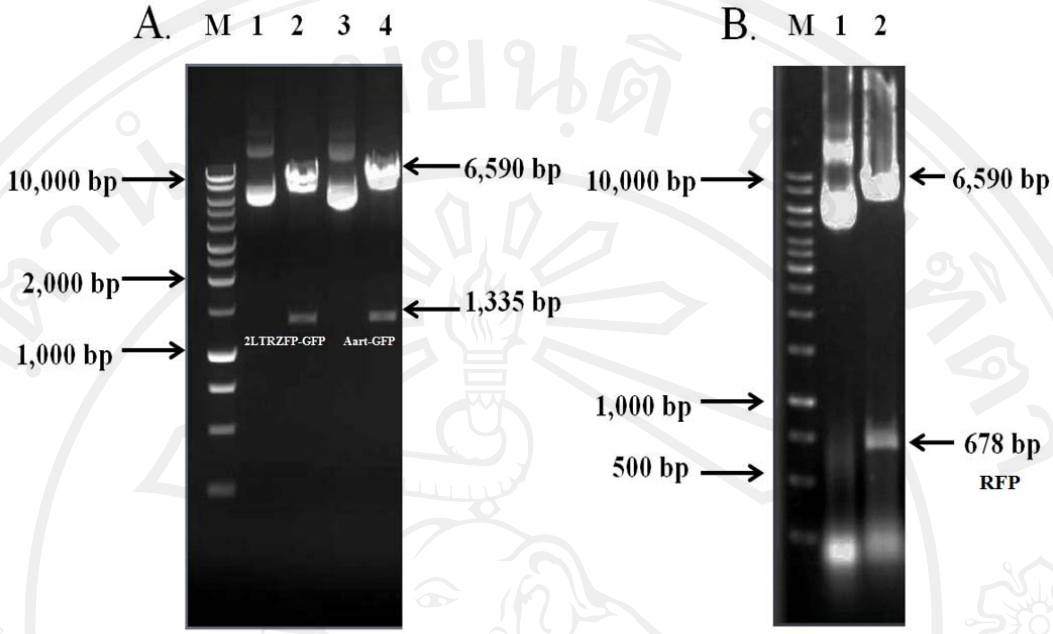

Figure 3.13 The restriction enzyme analysis of lentiviral-based vectors expressing for 2LTRZFP-GFP, Aart-GFP, and RFP.

(A) Lentiviral-based vectors were identified by restriction enzyme *Xba* I and *Sal* I.

lane M; molecular weight marker

lane 1; uncut pRRLSIN.cPPT.mPGK.2LTRZFP-GFP.WPRE

lane 2; cut pRRLSIN.cPPT.mPGK.2LTRZFP-GFP.WPRE

lane 3; uncut pRRLSIN.cPPT.mPGK.Aart-GFP.WPRE

lane 4; cut pRRLSIN.cPPT.mPGK.Aart-GFP.WPRE

(B) The restriction analysis of pRRLSIN.cPPT.mPGK-RFP.WPRE was identified by restriction enzyme *Xba* I and *Sal* I.

lane M; molecular weight marker

lane 1; uncut pRRLSIN.cPPT.mPGK-RFP.WPRE

lane 2; cut pRRLSIN.cPPT.mPGK-RFP.WPRE

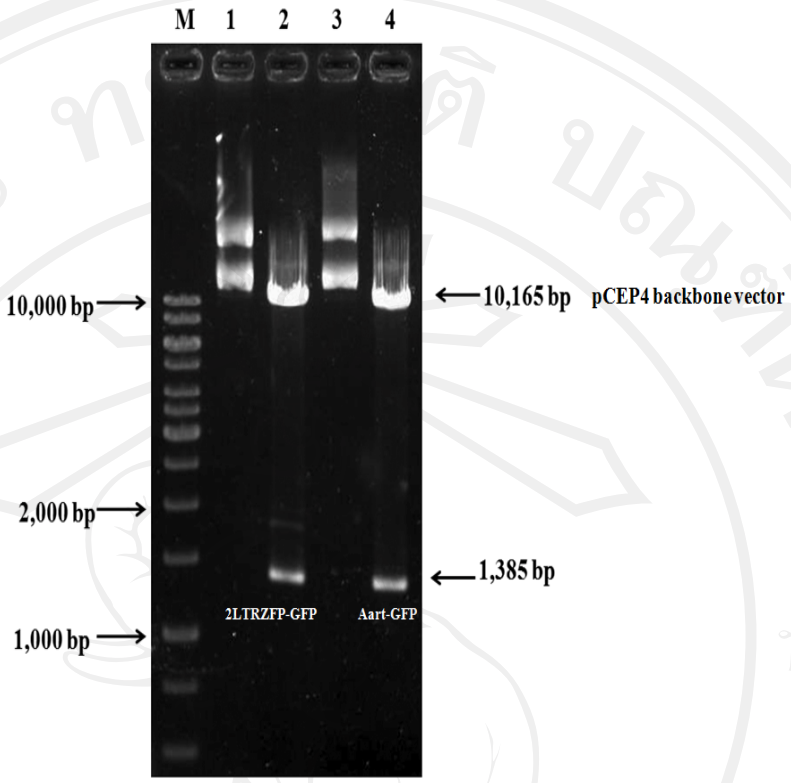

Figure 3.14 The restriction analysis of vector pCEP4-2LTRZFP-GFP and pCEP4-Aart-GFP. Vector pCEP4-2LTRZFP-GFP and pCEP4-Aart-GFP were analysed by restriction enzyme *Nhe*I and *Not*I.

lane M; molecular weight marker

lane 1; uncut pCEP4-2LTRZFP-GFP

lane 2; cut pCEP4-2LTRZFP-GFP

lane 3; uncut pCEP4-Aart-GFP

lane 4; cut pCEP4-Aart-GFP

Table 3.3 The results of p24 Ag and viral load assay in a production of VSV-G pseudotyped lentiviruses containing 2LTRZFP-GFP, Aart-GFP, and RFP.

VSV-G pseudotyped lentivirus	P 24 Ag (ng/ul)	Viral load (copies/ml)
2LTRZFP-GFP	4.4×10^3	25×10^6
Aart-GFP	5.6×10^3	30×10^6
RFP	2.9×10^3	12×10^6

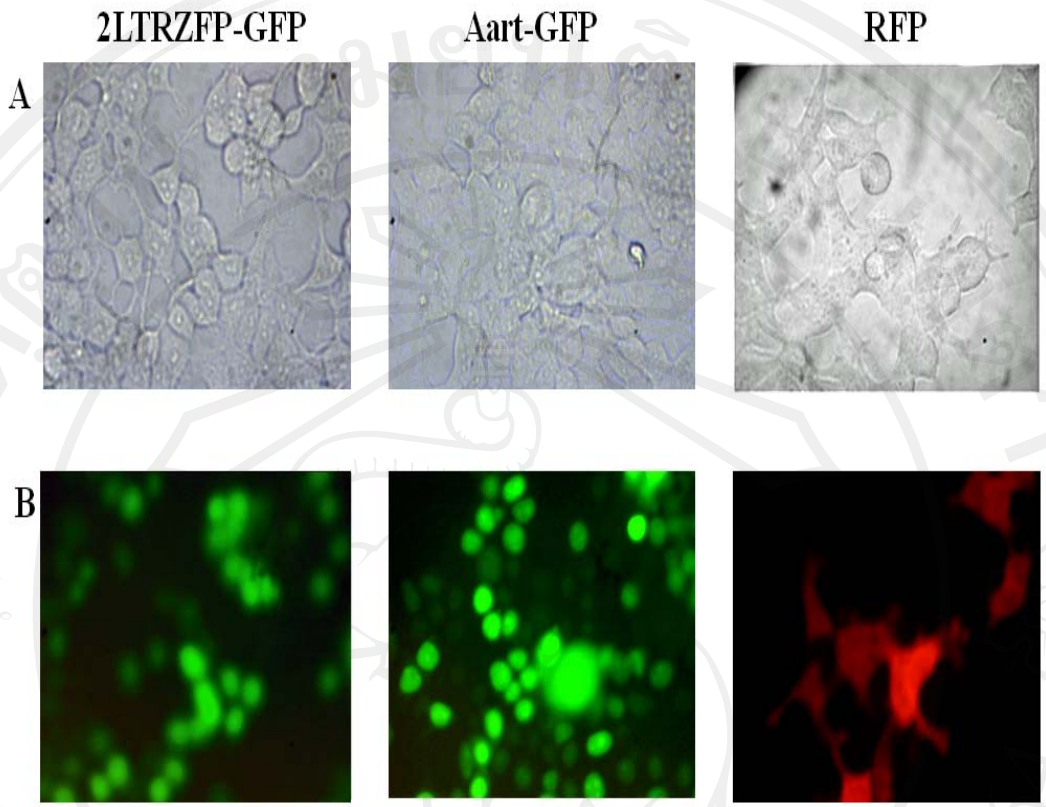

Figure 3.15 Expression of 2LTRZFP-GFP, Aart-GFP, and RFP in 293T cells. Stable 293T cell lines were created by transducing cells with pseudotyped lentivirus containing 2LTRZFP-GFP, Aart-GFP, and RFP. Expression was visualised by inverted fluorescent microscopy. Each stable line was imaged at 400× magnification in the same field. **(A)** Light-inverted channel. **(B)** Fluorescent channel**.**

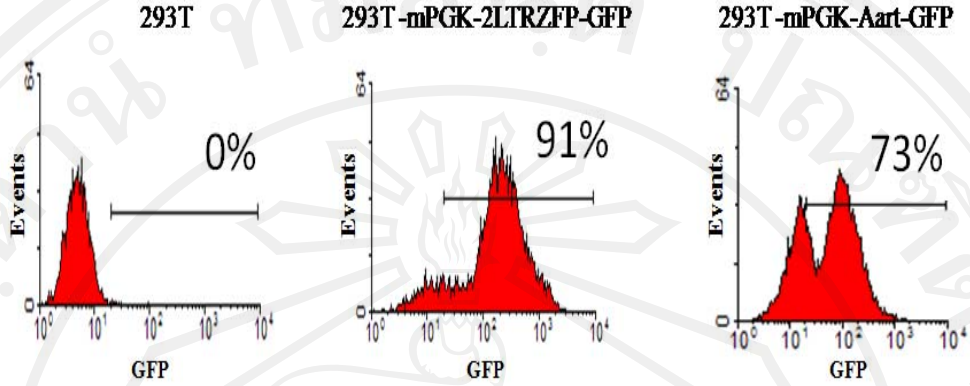

Figure 3.16 Long term expression of 2LTRZFP-GFP and Aart-GFP in 293T cells. Stable lines expression on day-90 of 293T transduced with pseudotyped lentivirus 2LTRZFP-GFP and Aart-GFP were analyzed for GFP by flow cytometer.

3.9 2LTRZFP-GFP inhibits VSV-G pseudotyped lentiviral RFP integration in 293T cells

The inhibition of VSV-G pseudotyped lentiviral RFP integration was studied in 293T cells stably transfected with either 2LTRZFP-GFP or Aart-GFP as shown in **Figure 3.17**. The cells were subcultured every 2 days after the challenge. The percentage of cells positive for RFP and GFP (upper right quadrant) was determined by flow cytometry to yield the proportion of GFP^+ cells infected with VSV-G pseudotyped RFP lentivirus in one round of infection. The 2LTRZFP-GFP cells inoculated with VSV-G pseudotyped RFP lentivirus at either 1 or 10 MOI had dramatically reduced RFP expression compared to the expression in Aart-GFP control cells. RFP expression in both 2LTRZFP-GFP and Aart-GFP cells decreased during the experimental time course for up to 45 days post-challenge due to the degradation of the unintegrated form of viral DNA (Butler et al., 2002; Zhou et al., 2005; Kelly et al., 2008). Similar results were obtained using confocal microscopy. The cells were stained with DAPI to visualise the nuclei as demonstrated in **Figure 3.18**.

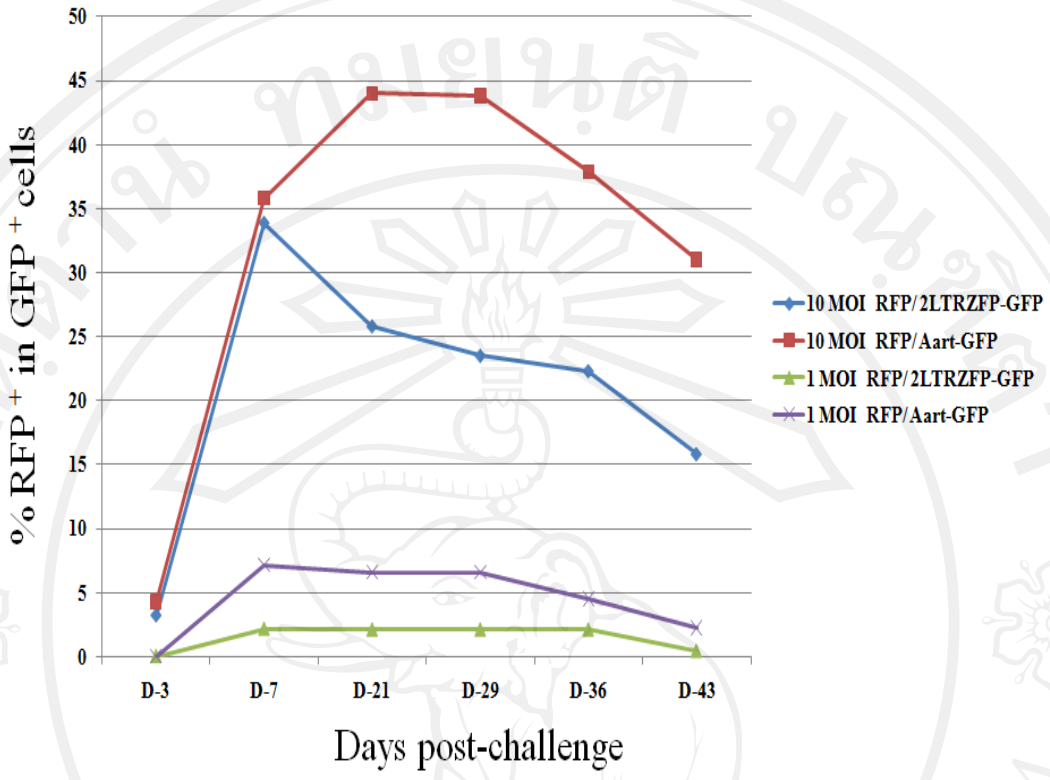

Figure 3.17 Inhibition of VSV-G pseudotyped lentiviral RFP expression by 2LTRZFP-GFP. 293T cells stably transfected with 2LTRZFP-GFP and Aart-GFP were challenged with VSV-G pseudotyped lentiviral RFP at 1 and 10 MOI. RFP expression in GFP^+ cells was determined by flow cytometry on days 3, 7, 21, 29, 36, and 43 after the challenge. Approximately 100,000 cells were gated per data point. This graph is representative of two independent experiments.

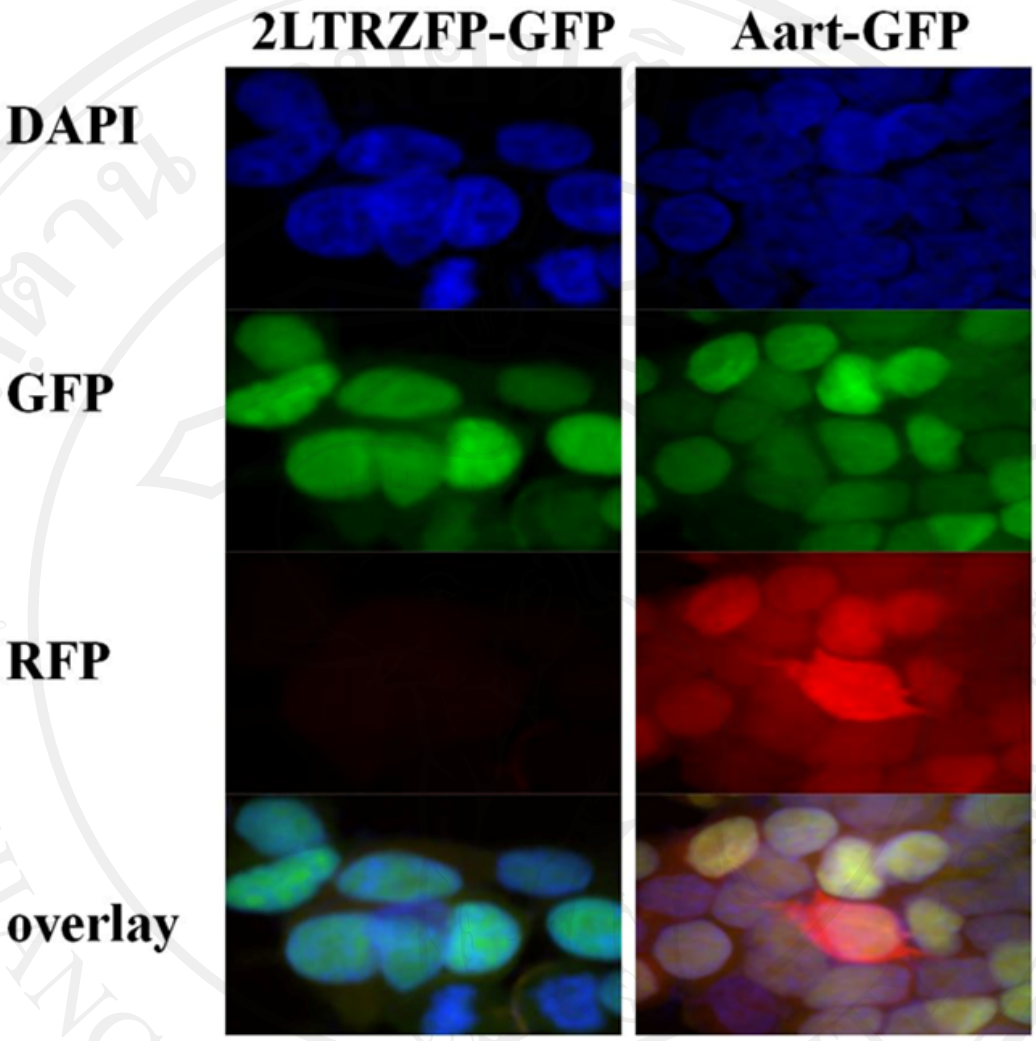

Figure 3.18 RFP expression in cells stably transfected with either 2LTRZFP-GFP or Aart-GFP. The cells that expressed 2LTRZFP-GFP or Aart-GFP were challenged with pseudotyped RFP lentivirus at 10 MOI. Twenty-nine days after the challenge, the cells were stained with DAPI to observe the nuclei, and they were visualised in the same field by confocal microscopy in DAPI, GFP, and RFP channels. The bottom row is the overlay image. The original magnification was 100×.

3.10 2LTRZFP-GFP inhibits HIV-1 replication in viral-transduced SupT1 cell line

SupT1 and SupT1 cells transduced with 2LTRZFP-GFP and Aart-GFP were analyzed for the efficiency of transduction represented by the percentage of GFP positive cells and mean fluorescence intensity (MFI) by flow cytometry. The results of % GFP positive were 0.6, 97.3, 56.9, and 98.5%, whereas MFI were 2.54, 35.14, 16.23, and 36.30 for non-transduced SupT1 cells, Aart-10F, ZFP-5E3, and ZFP-4F6 transduced SupT1 stable lines, respectively (**Figure 3.19**). All stable cells were checked CD4 expression on cell-surface by staining with purified anti-CD4 mAb, and they were greater than 97% as seen in **Figure 3.20**. These cells were infected with HIV-1_{NL4-3} at 0, 1, and 5 MOI. HIV-1 replication was monitored by quantifying the amount of p24 antigen released into the culture supernatants. At an MOI of 1 on day 13 after the challenge (**Figure 3.21)**, low levels of p24 antigen were observed in the supernatant of ZFP-4F6 cells, and a slightly higher level of HIV-1 p24 antigen was observed in the supernatant of ZFP-5E3 cells. Supernatants from controls (non-tranduced SupT1 cells and Aart-10F-transduced cells) had high levels of p24 antigen. At an MOI of 5, the level of HIV-1 p24 antigen in these supernatants was saturated due to over load of infection.

A qPCR assay was performed on extracted genomic DNA from stably transduced cell lines that were infected with HIV-1_{NL4-3} at a MOI of 1 on day 13 after the challenge (**Figure 3.22A, and B**). The mean cycle thresholds (C_ts) ± standard deviation (SD) of *Alu-gag* qPCR of DNA extracted from SupT1, Aart-10F, ZFP-5E3, and ZFP-4F6 cells were 27.5 ± 0.5, 28.4 ± 0.1, 34.3 ± 0.3, and 38.3 ± 0.3,

respectively, and the mean C_ts ± SD of *GAPDH* qPCR of these clones were similar with values of 22.4 ± 1.4, 23.1 ± 0.2, 23.9 ± 0.3, and 23.1 ± 0.7, respectively (**Figure 3.22**C). These results indicated that the presence of ZFP-5E3 or ZFP-4F6 inhibited the integration process and that no inhibition of HIV-1 integration was observed in the control cells.

Since the using method to generate the stable line was delivered by VSV-G pseudotyped lentivirus which it also integrated in to the host chromosome. *Alu* primer was used as a forward primer for amplifying integrated HIV DNA both HIV-1 pNL_{4-3} and VSV-G pseudotyped lentivirus. To diffentiate the integration between HIV-1 pNL_{4-3}, and VSV-G pseudotyped lentivirus, a specific primer was designed to bind only in *gag* region of HIV-1 pNL_{4-3}, whereas this primer cannot bind a truncated *gag* region in VSV-G pseudotyped lentivirus. However, a specific primer to truncated *gag* region in VSV-G pseudotyped lentivirus was designed to amplify a background of transduction. A qPCR assay was performed on extracted genomic DNA from stably transfected cell lines that were infected with HIV-1_{NL4-3} at 1 MOI on day 13 after the challenge (**Figure 3.23A, and B**). The cycle thresholds (C_ts) of *Alu-gag* qPCR for pNL_{4-3} of DNA extracted from SupT1, Aart-10F, ZFP-5E3, and ZFP-4F6 were 27.2, 28.0, 34.6, and 39.2, respectively, whereas *Alu-gag* qPCR for lentivirus were similar 21.0, 21.9, 19.7, and 21.2, respectively. The C_ts of GAPDH qPCR of these clones were similar 23.1, 24.1, 24.6, and 24.0, respectively (**Figure 3.23C**).

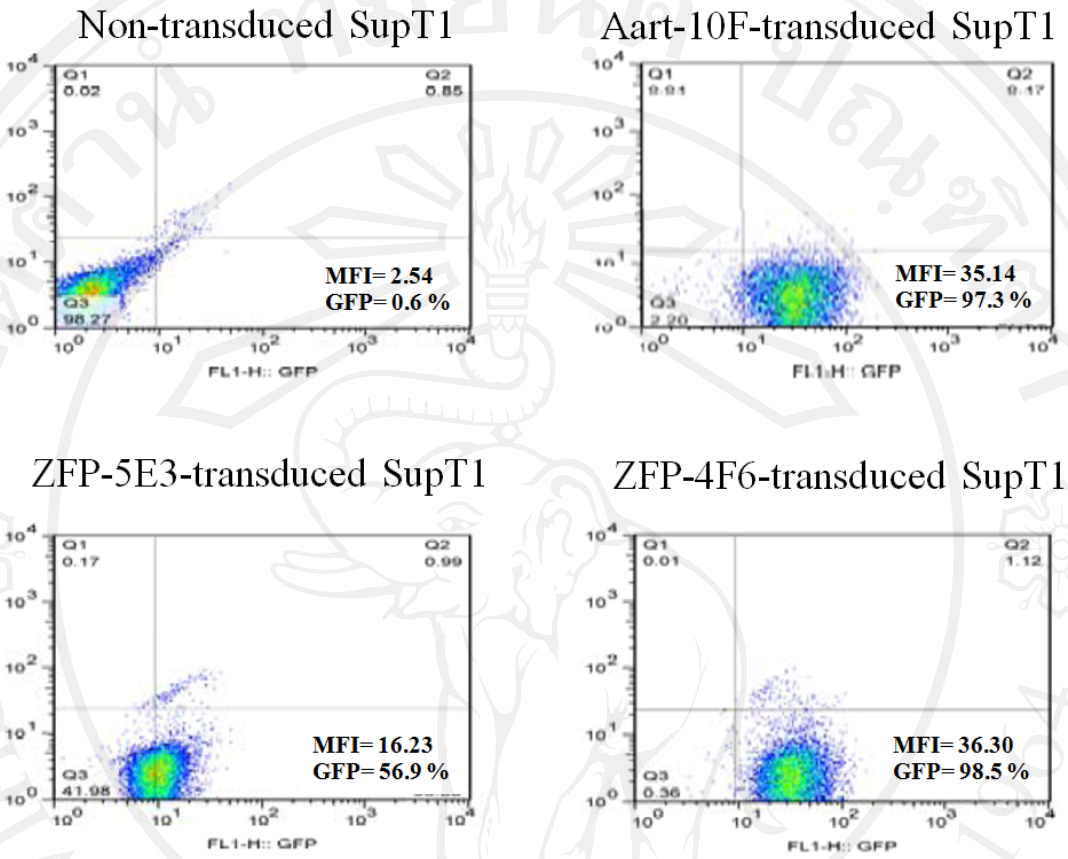

Figure 3.19 GFP expression in SupT1 cells stably transduced with either 2LTRZFP-GFP or Aart-GFP. Cells that expressed 2LTRZFP-GFP or Aart-GFP were monitored GFP by flow cytometry. MFI; mean fluorescence intensity.

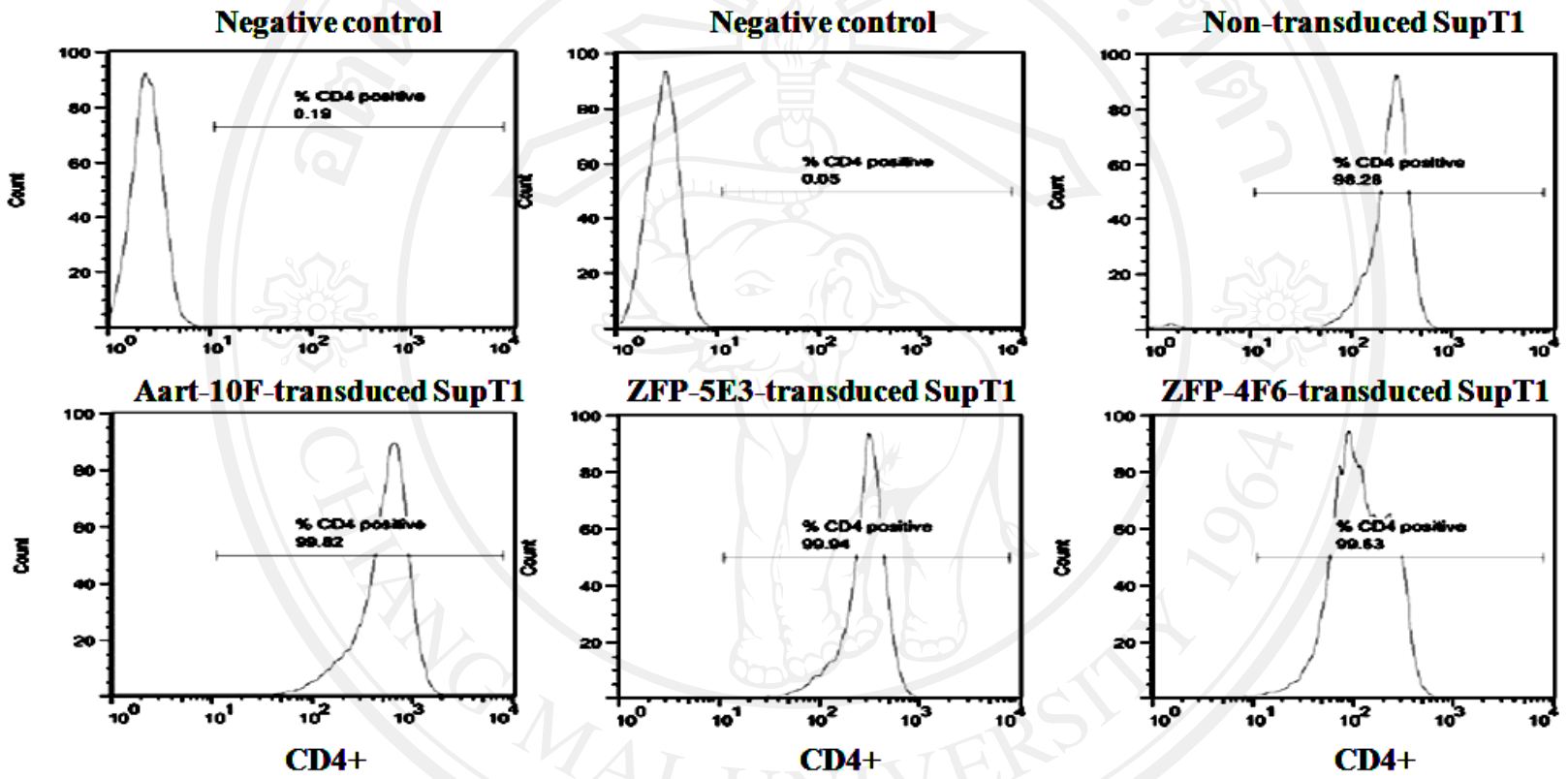

Figure 3.20 CD4 expression on the surface of cells stably transduced with either 2LTRZFP-GFP or Aart-GFP.

Cells that expressed 2LTRZFP-GFP or Aart-GFP were stained with purified anti-CD4 mAb and analyzed by flow cytometry.

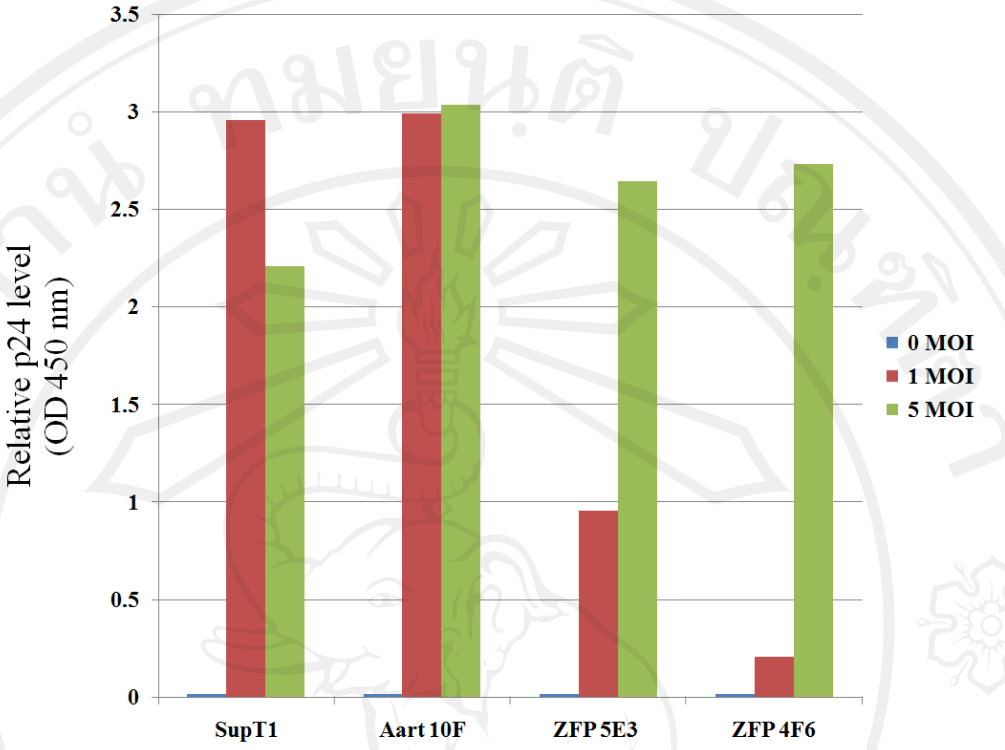

Figure 3.21 A comparison of HIV-1 p24 Ag in culture supernatants of each stably transduced with either 2LTRZFP-GFP or Aart-GFP after infection. SupT1 cells were transduced with either 2LTRZFP-GFP or Aart-GFP using third-generation lentiviral expression vectors. The following stable lines were propagated: Aart-10F, ZFP-5E3, and ZFP-4F6. These cells were infected with HIV-1_{NL4-3} at 0, 1, and 5 MOI. HIV-1 p24 Ag in culture supernatants of these cells on day 13 after the challenge was determined by using Genetic Systems HIV-1 Ag EIA kit. This graph is representative of two independent experiments.

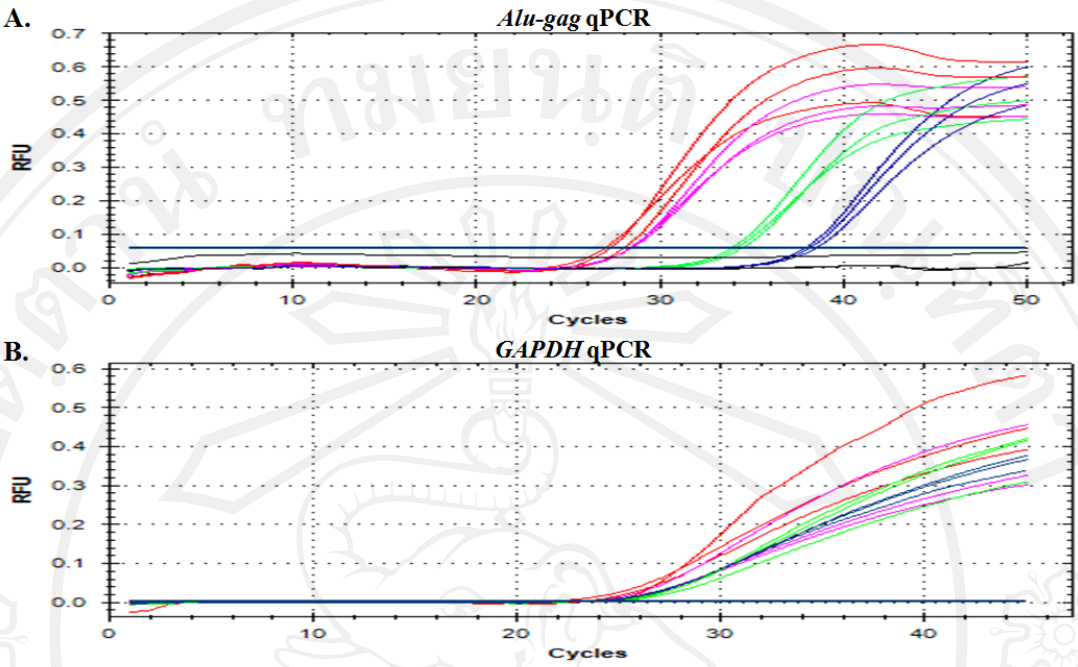

C.

	SupT1	Aart 10F	ZFP 5E3	ZFP4F6
Alu-gag qPCR	27.5 ± 0.5	28.4 ± 0.1	34.3 ± 0.3	38.3 ± 0.3
GAPDH qPCR	22.4 ± 1.4	23.1 ± 0.2	23.9 ± 0.3	23.1 ± 0.7

Figure 3.22 The relative inhibition of HIV-1 integration in stably transduced SupT1 with 2LTRZFP-GFP by *Alu-gag* qPCR. HIV-1 DNA in extracted genomic DNA from SupT1 cells stably transduced with either 2LTRZFP-GFP or Aart-GFP on day 13 after the challenge was amplified by *Alu-gag* qPCR. **(A)** *Alu-gag* qPCR **(B)** *GAPDH* qPCR **(C)** The mean cycle thresholds (C_ts) of *Alu-gag* qPCR and *GAPDH* qPCR in each stable line were designated in red, purple, green, dark blue for SupT1, Aart 10F, ZFP-5E3, and ZFP-4F6, respectively. The PCR assays were performed in triplicate.

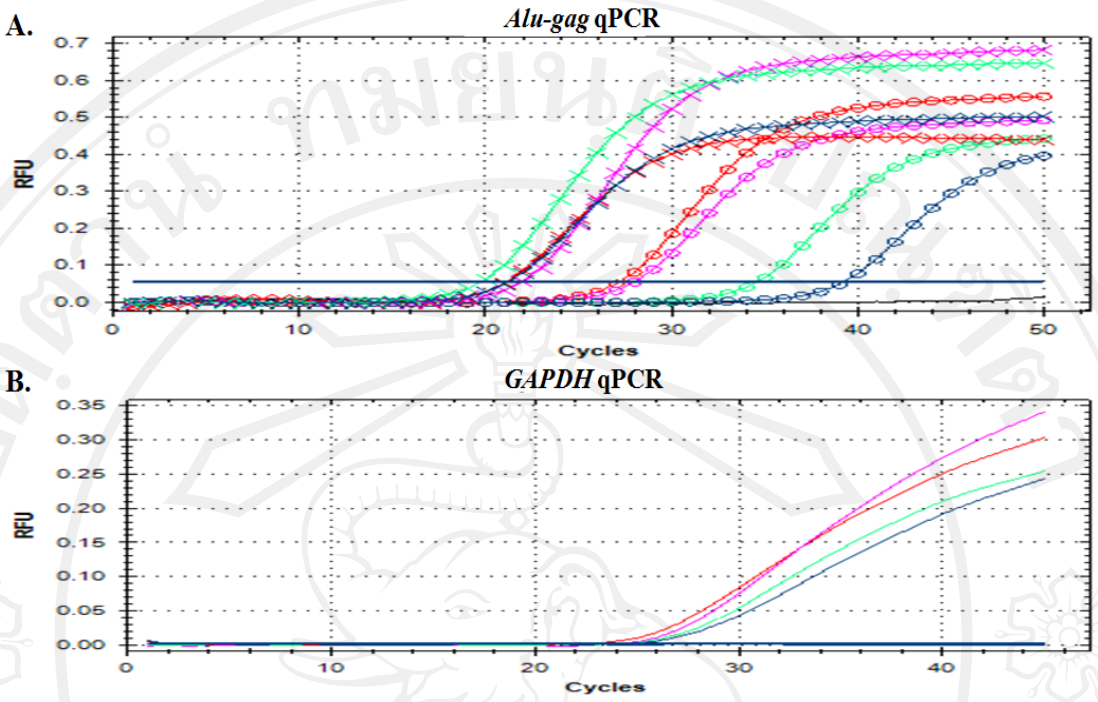

C.

	SupT1	Aart-10F	ZFP-5E3	ZFP-4F6
Alu-gag qPCR (pNL_{4-3})	27.2	28.0	34.6	39.2
Alu-gag qPCR (lentivirus)	21.0	21.9	19.7	21.2
GAPDH qPCR	23.1	24.1	24.6	24.0

Figure 3.23 Differentiation between HIV-1 and VSV-G pseudotyped lentivirus integration by *Alu-gag* qPCR. HIV-1 DNA in extracted genomic DNA from SupT1 cells stably transduced with either 2LTRZFP-GFP or Aart-GFP on day 13 after the challenge was amplified by *Alu-gag* qPCR. **(A)** *Alu-gag* qPCR for pNL_{4-3} (O—O) and *Alu-gag* qPCR for lentivirus (><—><) **(B)** *GAPDH* qPCR **(C)** The cycle thresholds (C_ts) of *Alu-gag* qPCR and *GAPDH* qPCR in each stable line were designated in red, purple, green, dark blue for SupT1, Aart-10F, ZFP-5E3, and ZFP-4F6, respectively.

3.11 Inhibition of HIV-1 replication in non-viral transfected SupT1 expressing 2LTRZFP-GFP

SupT1 cells were electrotransfected with the pCEP4-2LTRZFP-GFP and pCEP4-Aart-GFP vectors to produce stable lines. These cells were continuously selected by limiting dilution in hygromycin B. Flow cytometry analysis showed that the transfection efficiencies based on the expression of GFP were more than 90%**,** whereas MFI were 2.36, 52.08, 110.90, 71.30 for non-transfected SupT1 cells, Aart-7G, ZFP-9B1, and ZFP-9B2 transfected SupT1 stable lines, respectively (**Figure 3.24)**, whereas the cell surface expressions of CD4 were greater than 90% (**Figure 3.25**). These cells were then infected with HIV-1_{NL4-3} at 0, 1, and 5 MOI. HIV-1 replication was determined by analysis of the p24 antigen released into the culture supernatants. On day 13 after the challenge, expression of ZFP-9B1 and ZFP-9B2 completely inhibited viral integration at both 1 and 5 MOI, and high levels of p24 antigen were observed in the supernatants of control SupT1 and Aart-7G cells (**Figure 3.26**). Protection due to expression of the ZFPs was observed throughout the experiment for up to 25 days post-challenge (**Figure 3.27**).

A qPCR assay was performed on extracted genomic DNA from stably transfected cell lines that were infected with HIV-1_{NL4-3} at a MOI of 5 on day 13 after the challenge (**Figure 3.28A, and B**).The mean C_ts ± SD of *Alu-gag* qPCR in non-transfected SupT1 cells and Aart-7G-transfected cells were 28.4 ± 0.4 and 27.0 ± 0.2, respectively, and no product was observed for cells transfected with either ZFP-9B1 or ZFP-9B2. The mean C_ts ± SD of *GAPDH* qPCR of these clones were comparable (24.5 ± 0.5, 24.6 ± 0.4, 25.6 ± 0.3, and 25.2 ± 0.2, respectively) (**Figure 3.28C**).

These results confirmed that ZFP-9B1 and ZFP-9B2 completely inhibited HIV-1 integration. Cell viability was monitored by trypan blue exclusion staining. All cell lines at all MOIs on day 13 after the challenge had almost 100% viability with the exception of non-transfected SupT1 cells and Aart-7G-transfected cells at a MOI of 5 (56 and 60% viability, respectively) (**Figure 3.29**). Syncytium formation, as indicated by arrows, resulting from cell-cell fusion mediated by viral infection was observed in control SupT1 and Aart-7G cells, but syncytium formation was not observed in ZFP-expressing cells due to the inhibition of the cytopathic effects by 2LTRZFP-GFP (**Figure 3.30**).

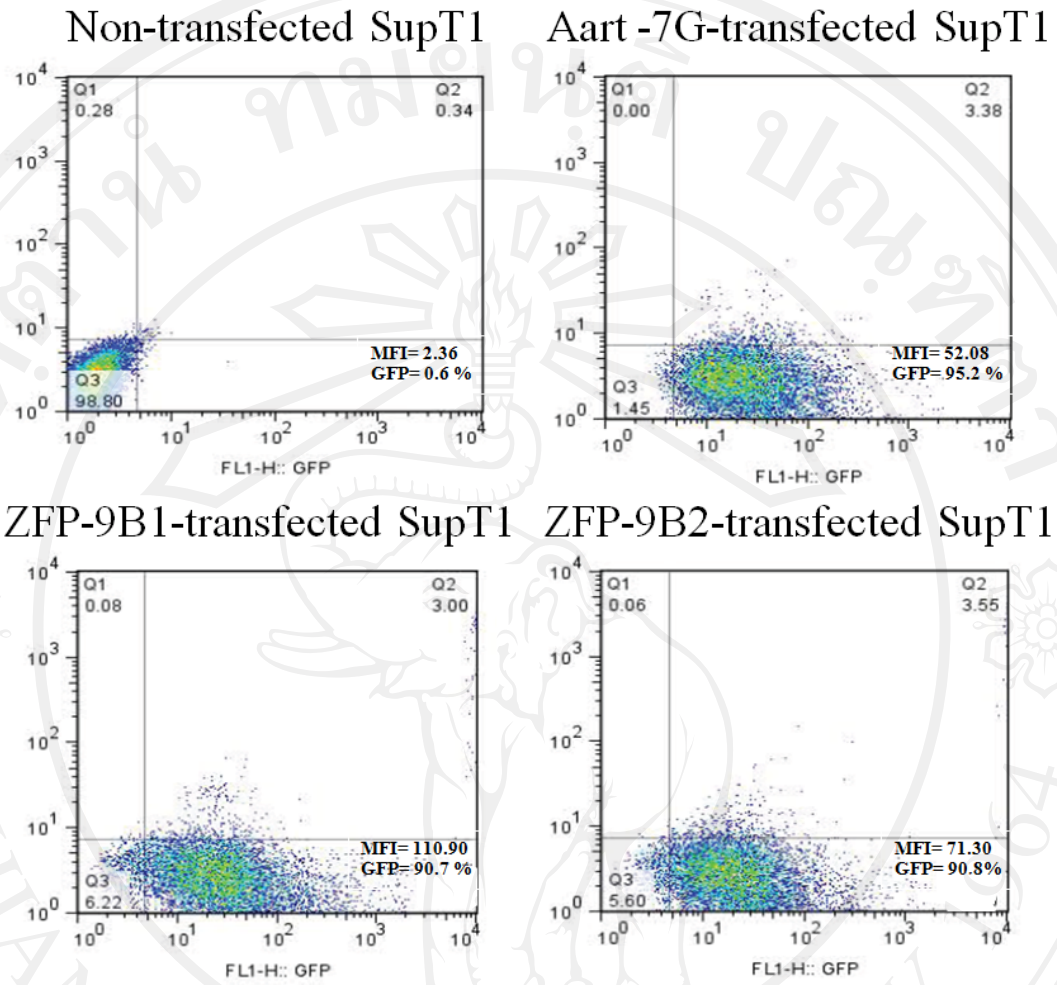

Figure 3.24 GFP expression in SupT1 cells stably transfected with either 2LTRZFP-GFP or Aart-GFP. Cells that expressed 2LTRZFP-GFP or Aart-GFP were monitored GFP by flow cytometry. MFI; mean fluorescence intensity.

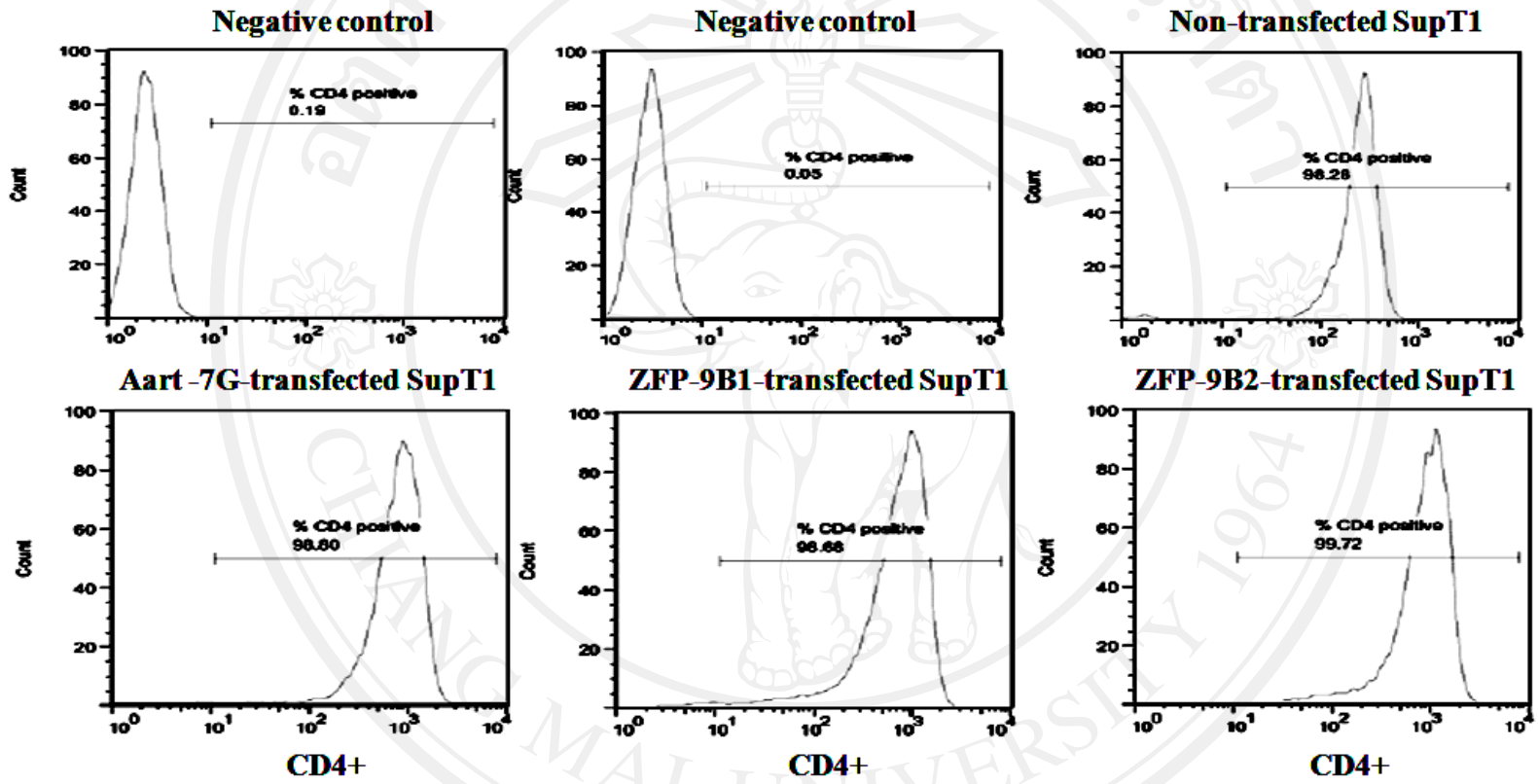

Figure 3.25 CD4 expression on the surface of cells stably transfected with either 2LTRZFP-GFP or Aart-GFP.

Cells that expressed 2LTRZFP-GFP or Aart-GFP were stained with purified anti-CD4 mAb and analyzed by flow cytometry.

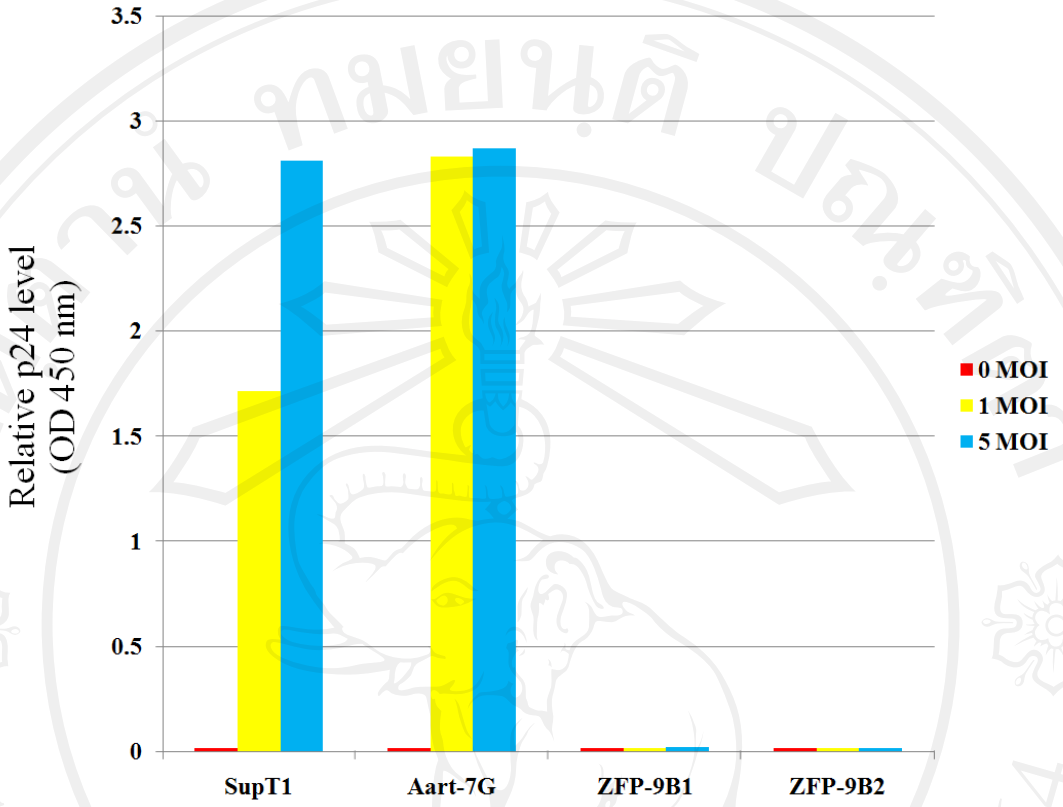

Figure 3.26 A comparison of HIV-1 p24 Ag in culture supernatants of each stably transfected with either 2LTRZFP-GFP or Aart-GFP after infection. SupT1 cells were transfected with either pCEP4-2LTRZFP-GFP vector or the pCEP4-Aart-GFP vector. The following stable lines were produced using selection under hygromycin B treatment: Aart-7G, ZFP-9B1, and ZFP-9B2. These cells were infected with HIV-1_{NL4-3} at 0, 1, and 5 MOI. HIV-1 p24 Ag in culture supernatants of these cells on day 13 after the challenge was determined by using Genetic Systems HIV-1 Ag EIA kit. This graph is representative of two independent experiments.

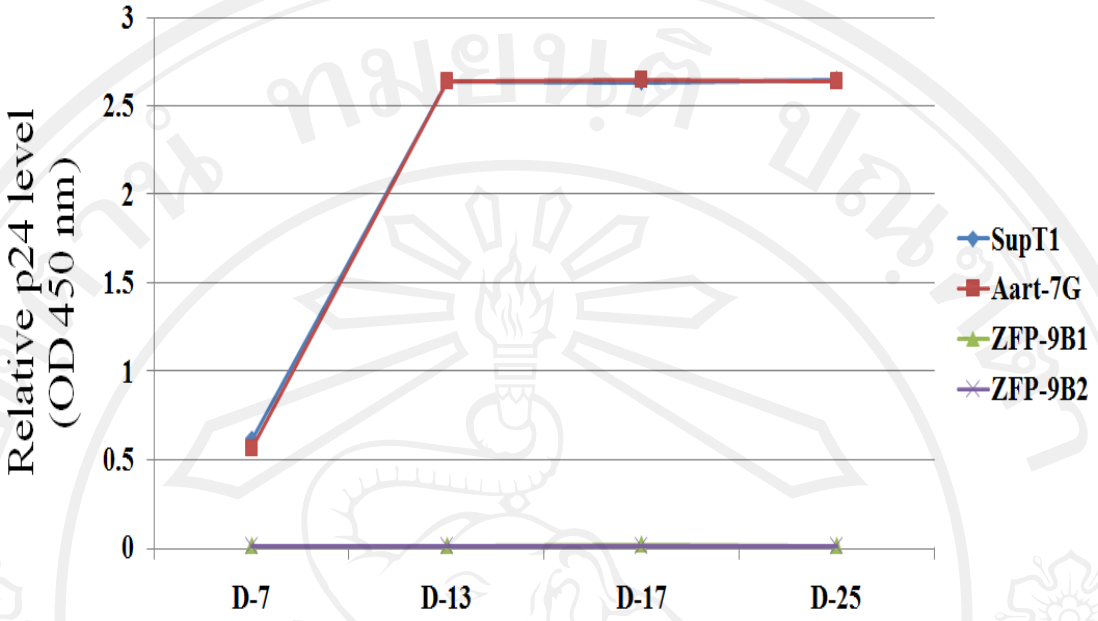

Figure 3.27 Inhibition of HIV-1 replication in 2LTRZFP-GFP-transfected T-lymphoid cells. Stable lines of transfected SupT1 cells with either 2LTRZFP-GFP or Aart-GFP were challenged with HIV-1_{NL4-3}. HIV-1 p24 Ag in supernatants from cells infected at 5 MOI on indicated days after the challenge was monitored by using Genetic Systems HIV-1 Ag EIA kit.

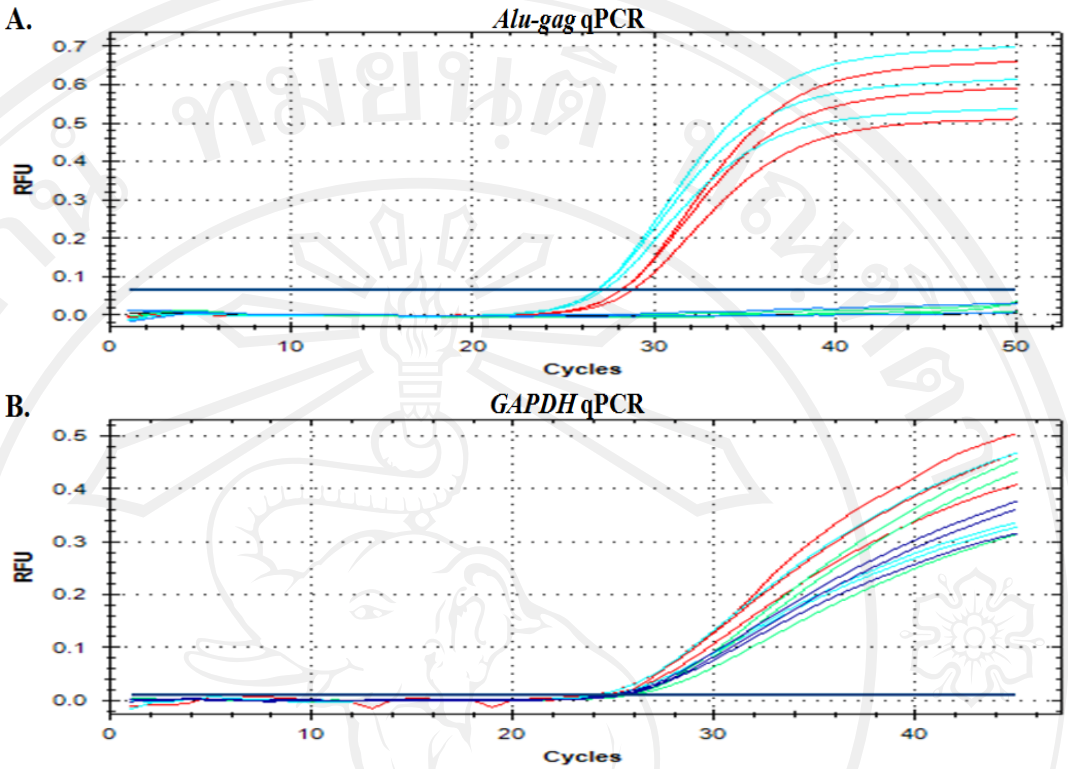

C.

	SupT1	Aart-7G	ZFP-9B1	ZFP-9B2
Alu-gag qPCR	28.4 ± 0.4	27.0 ± 0.2	NA	NA
GAPDH qPCR	24.5 ± 0.5	24.6 ± 0.4	25.6 ± 0.3	25.2 ± 0.2

Figure 3.28 The relative inhibition of HIV-1 integration in stably transfected SupT1 with 2LTRZFP-GFP by *Alu-gag* qPCR. Extracted genomic DNA from SupT1 cells stably transfected with either 2LTRZFP-GFP or Aart-GFP on day 13 after the challenge with HIV-1 at 5 MOI was amplified by *Alu-gag* qPCR. **(A)** *Alu-gag* qPCR **(B)** *GAPDH* qPCR **(C)** The mean cycle thresholds (C_ts) of *Alu-gag* qPCR and *GAPDH* qPCR in each stable line were designated in red, blue, green, dark blue for SupT1, Aart-7G, ZFP-9B1, and ZFP-9B2, respectively. NA: below detection threshold. The PCR assays were performed in triplicate.

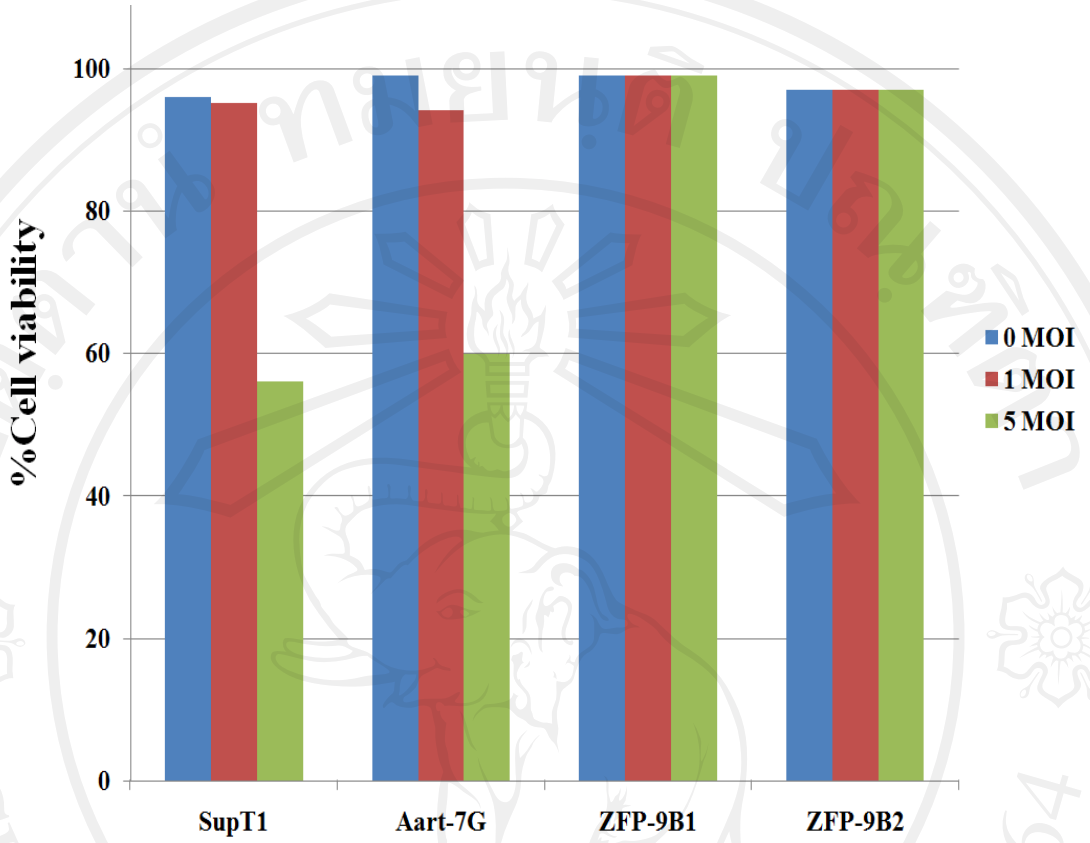

Figure 3.29 The percentage of cell viability in stably transfected SupT1 cells on day 13 after the challenge. SupT1 cells were transfected with either pCEP4-2LTRZFP-GFP vector or the pCEP4-Aart-GFP vector.These cells were infected with HIV-1_{NL4-3} at 0, 1, and 5 MOI. Cell viability of these cells on day 13 after the challenge was determined by trypan blue exclusion stain.

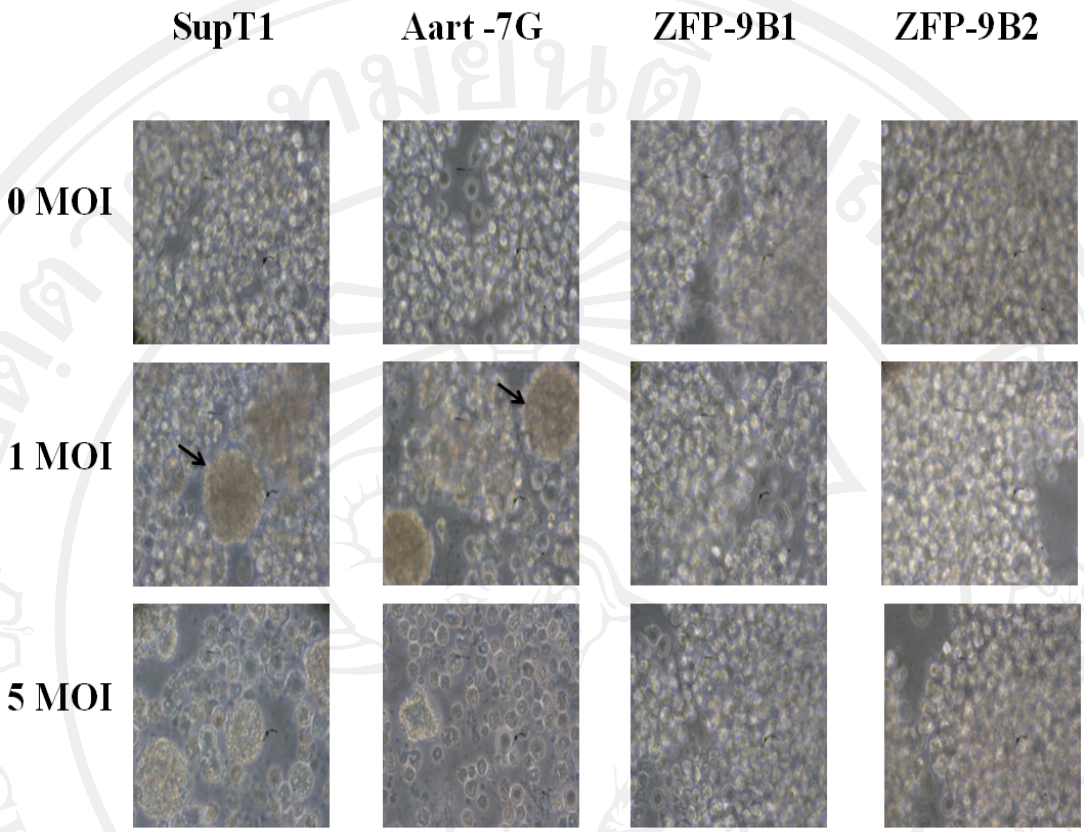

Figure 3.30 Inhibition of cytopathic effects by 2LTRZFP-GFP. SupT1 cells were transfected with either pCEP4-2LTRZFP-GFP vector or the pCEP4-Aart-GFP vector. These cells were infected with HIV-1_{NL4-3} at 0, 1, and 5 MOI. On day 13 after the challenge, the morphology of syncytium formations of cells indicated by arrow was imaged at 400× magnification by inverted microscopy.